Diffractive Optical Elements and Micro-Optics

이 병 호

서울대 전기공학부

byoungho@snu.ac.kr

OEQELab

Diffraction

Sommerfeld:

“any deviation of light rays from rectilinear paths which cannot be interpreted as reflection or refraction”

Examples of Fraunhofer Diffraction

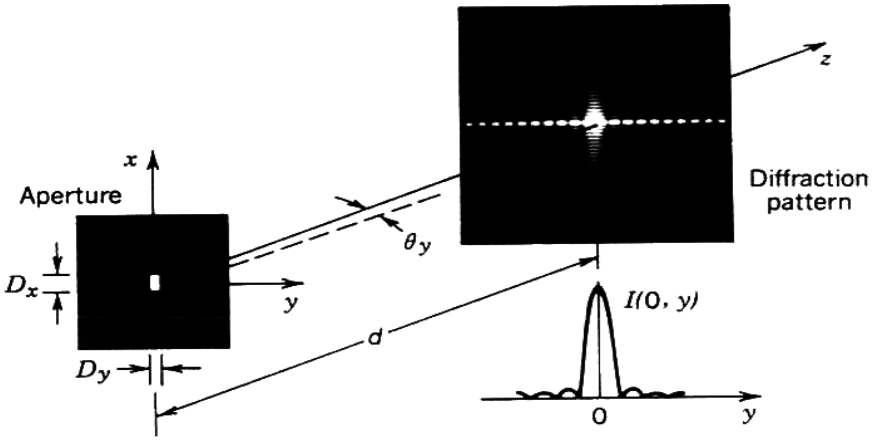

Fraunhofer diffraction from a rectangular aperture. The central lobe of the pattern has half-angular widths $\theta_x = \lambda / D_x$ and $\theta_y = \lambda / D_y$

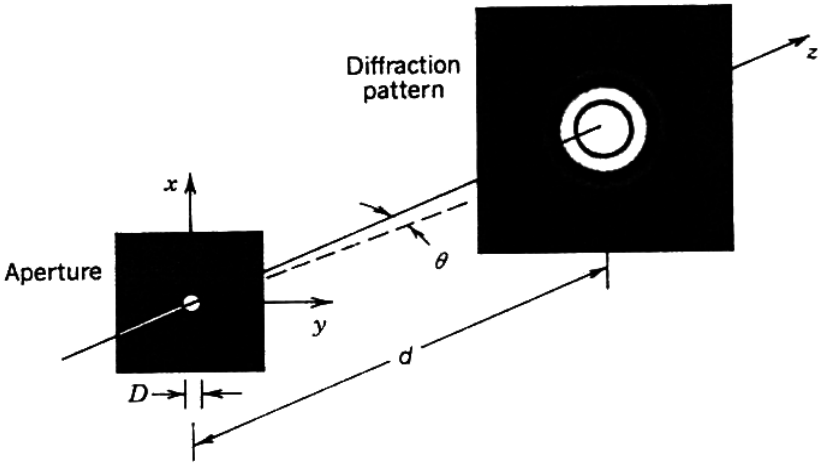

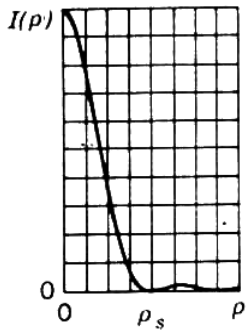

The Fraunhofer diffraction pattern from a circular aperture produces the Airy pattern with the radius of the central disk subtending an angle $\theta = 1.22\lambda / D$

Fresnel Diffraction by Square Aperture

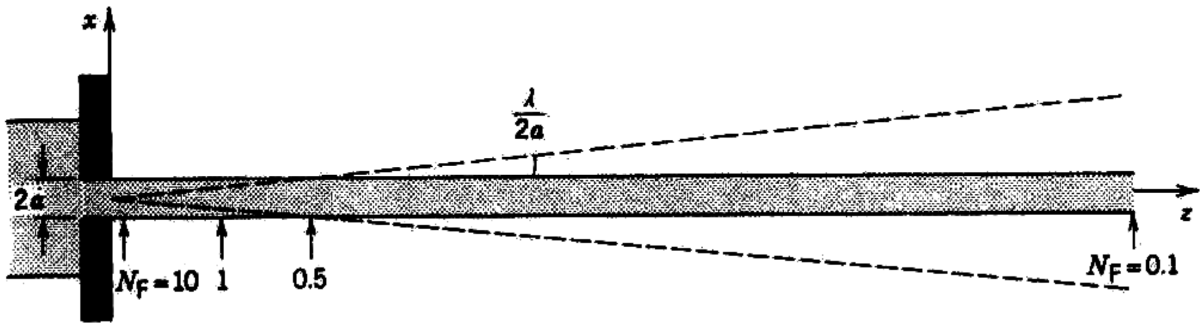

(a)

Fresnel Diffraction from a slit of width $D = 2a$. (a) Shaded area is the geometrical shadow of the aperture. The dashed line is the width of the Fraunhofer diffracted beam.

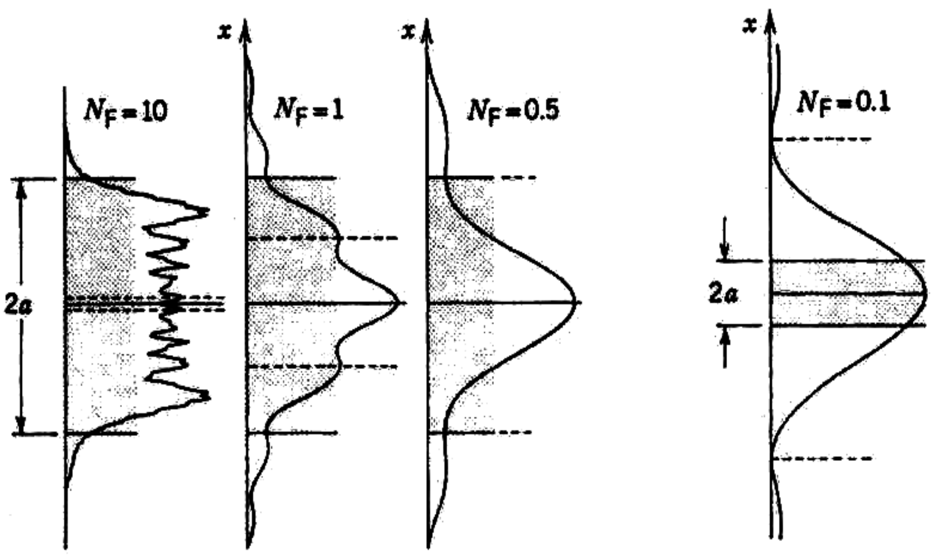

(b)

(b) Diffraction pattern at four axial positions marked by the arrows in (a) and corresponding to the Fresnel numbers N_F=10, 1, 0.5, and 0.1. The shaded area represents the geometrical shadow of the slit. The dashed lines at $|x| = (\lambda / D)d$ represent the width of the Fraunhofer pattern in the far field. Where the dashed lines coincide with the edges of the geometrical shadow, the Fresnel number $N_F = a^2 / \lambda d = 0.5$.

Diffractive Optics Technology

Provides new degrees of freedom for the design and optimization of optical systems

❑ Features

- ✓ **Large aperture, lightweight optical elements**
- ✓ **Aberration correction and achromatization**
- ✓ **Eliminates need for exotic materials**
- ✓ **Increase in performance over conventional systems**
- ✓ **System weight, complexity, and cost can be reduced significantly**

❑ Applications

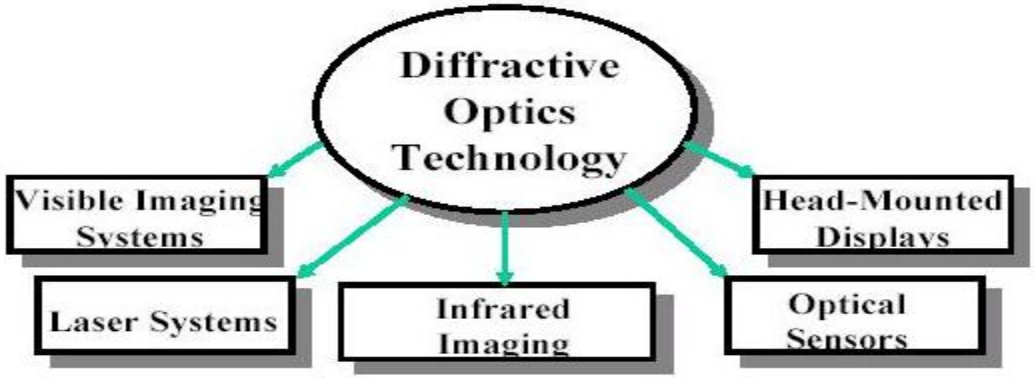

Fabrication of a Surface-Relief Master

- **Lithography – Optical & E-Beam**
  - ✓ Staircase blaze profiles
    - Binary optics – multiple e-beam masks
  - ✓ Continuous blaze profiles
    - Gray-scale masks
    - Variable e-beam exposure
- **Single-Point Diamond Turning**
  - ✓ Linear and spherical blaze profiles
- **Single-Point Laser Pattern Generation**
  - ✓ Vary exposure to shape blaze profile
  - ✓ X-Y and R-theta scan geometries

Diffractive Optical Element (DOE) (I)

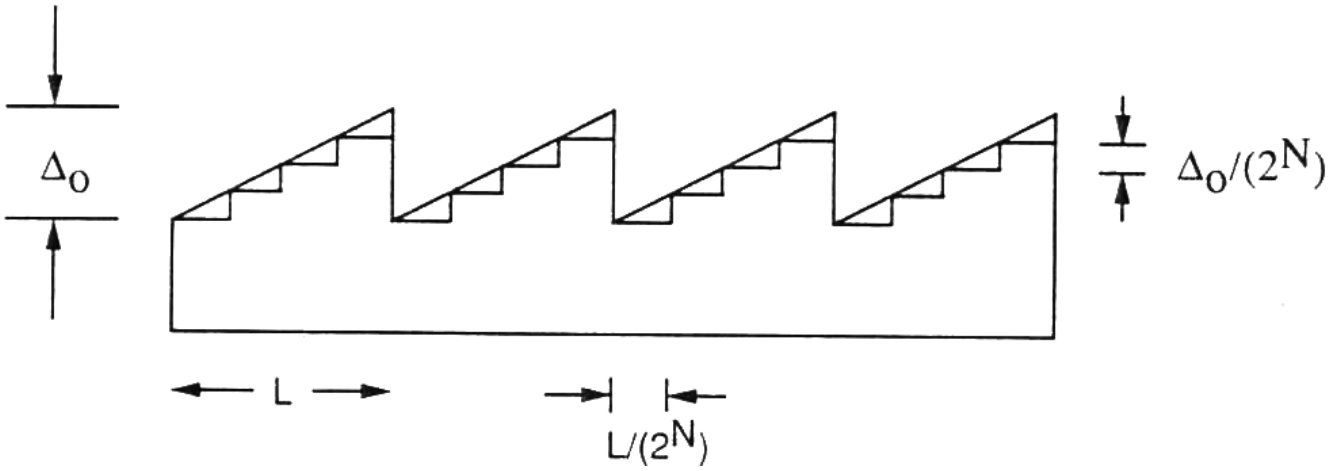

$$\eta_q = \mathrm{sinc}^2\left(\frac{q}{2^N}\right)\frac{\mathrm{sinc}^2\left(q-\frac{\phi_0}{2\pi}\right)}{\mathrm{sinc}^2\left(\frac{q-\frac{\phi_0}{2\pi}}{2^N}\right)}$$

Diffractive Optical Element (DOE) (II)

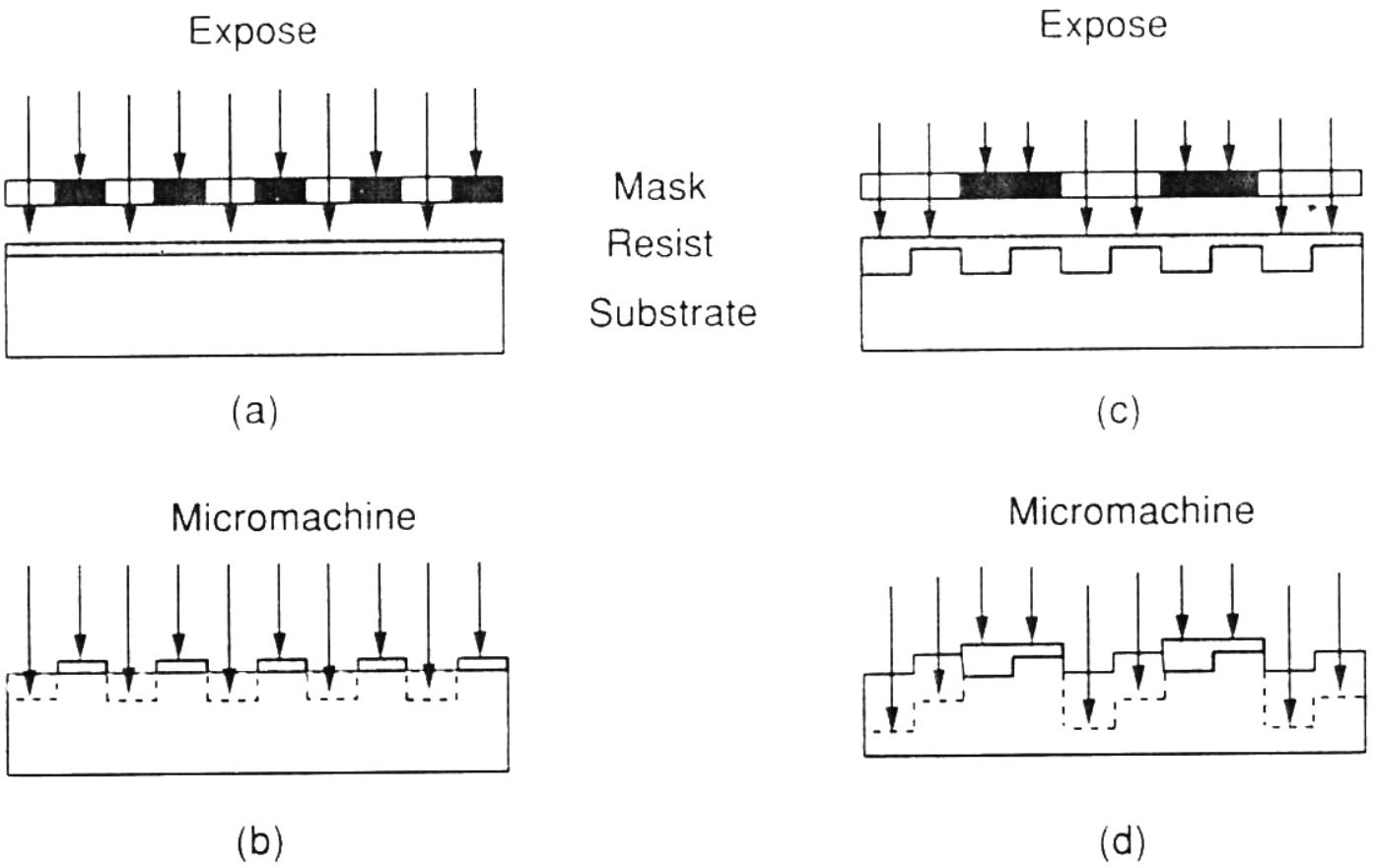

Advances in Single-Point Diamond Turning

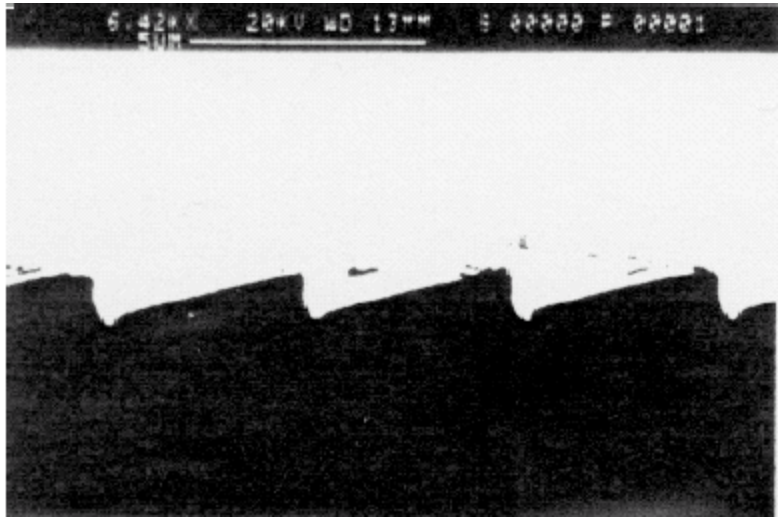

1989

Diffraction Efficiency

η : 85% - 90%

1999

Diffraction Efficiency

η : 97% - 99%

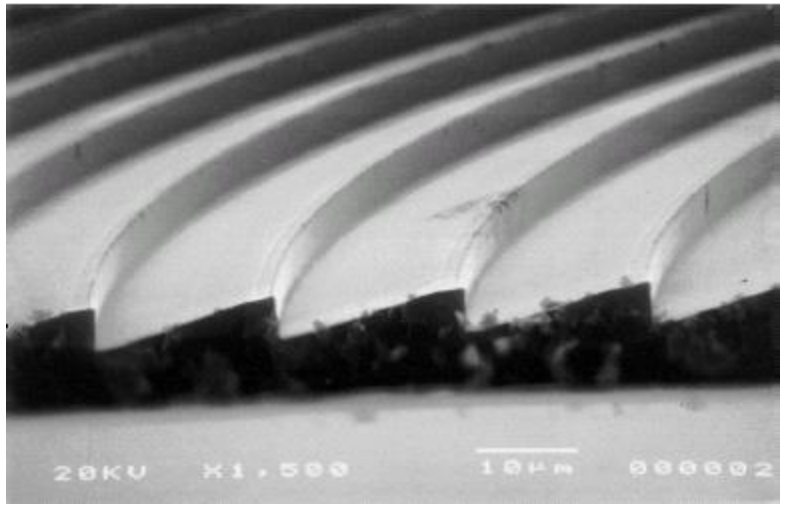

G. M. Morris

Laser Pattern Generator

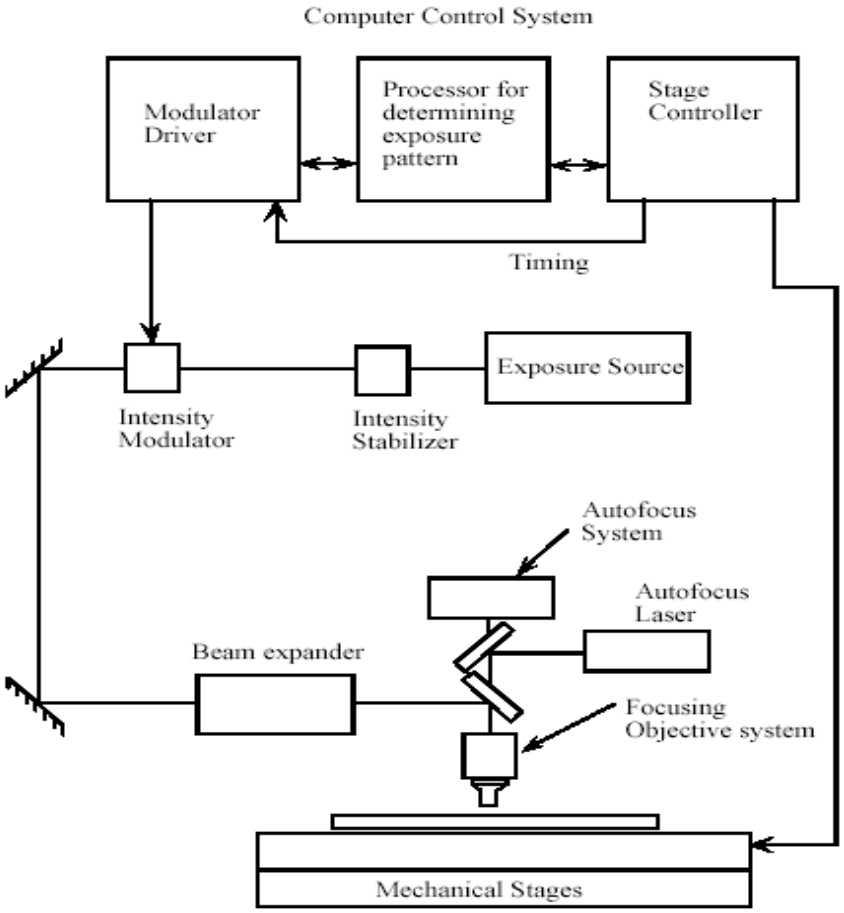

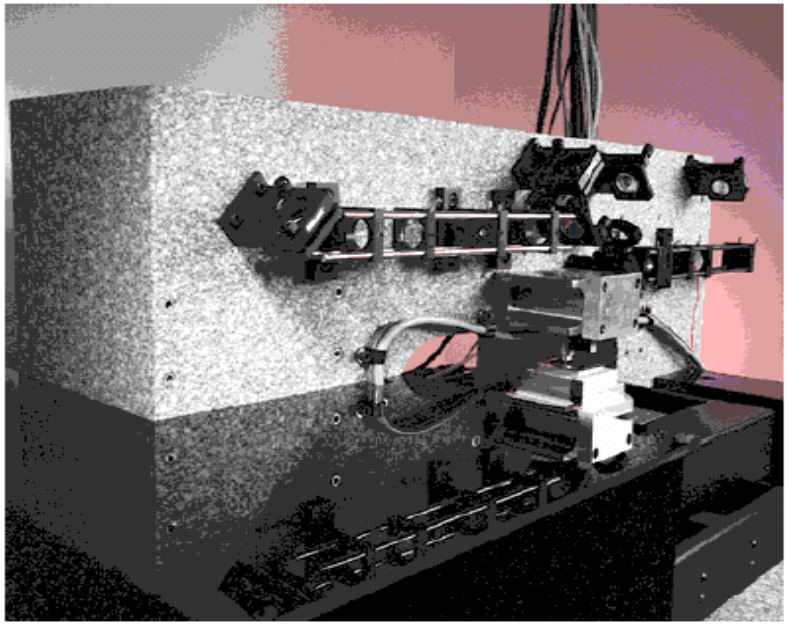

G. M. Morris

Micro-Optics Manufacturing Technique using Reactive Ion Etching

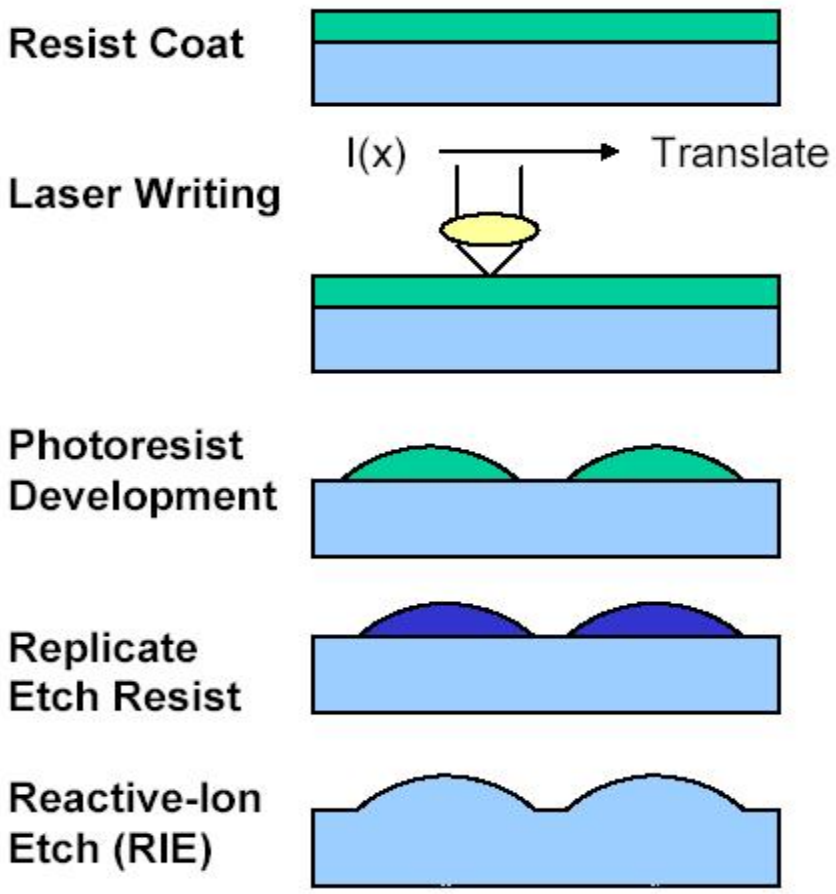

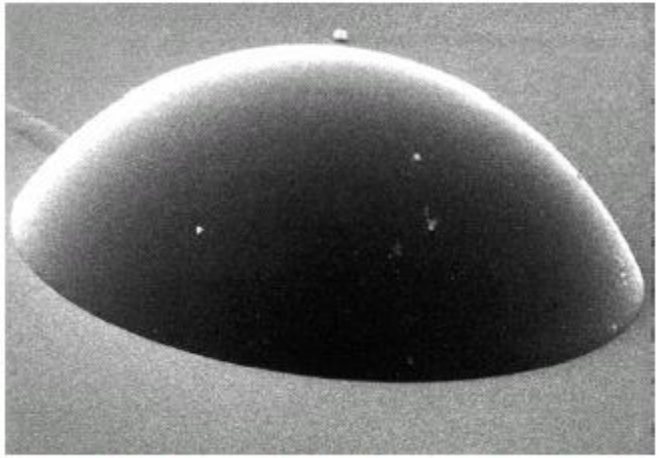

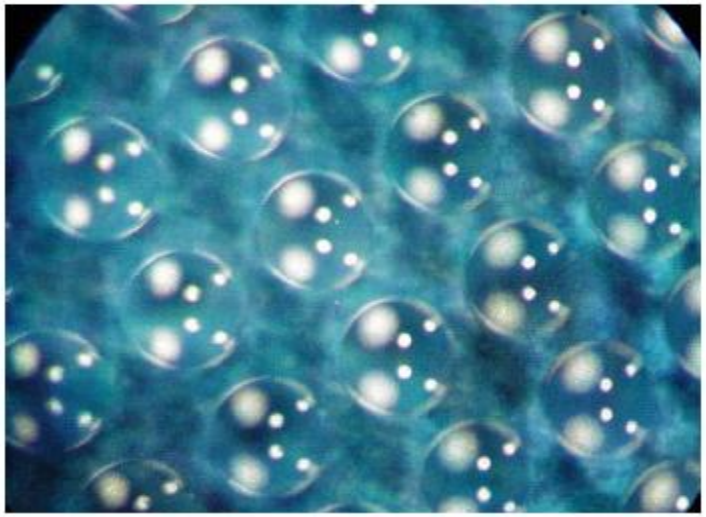

Microlens (I)

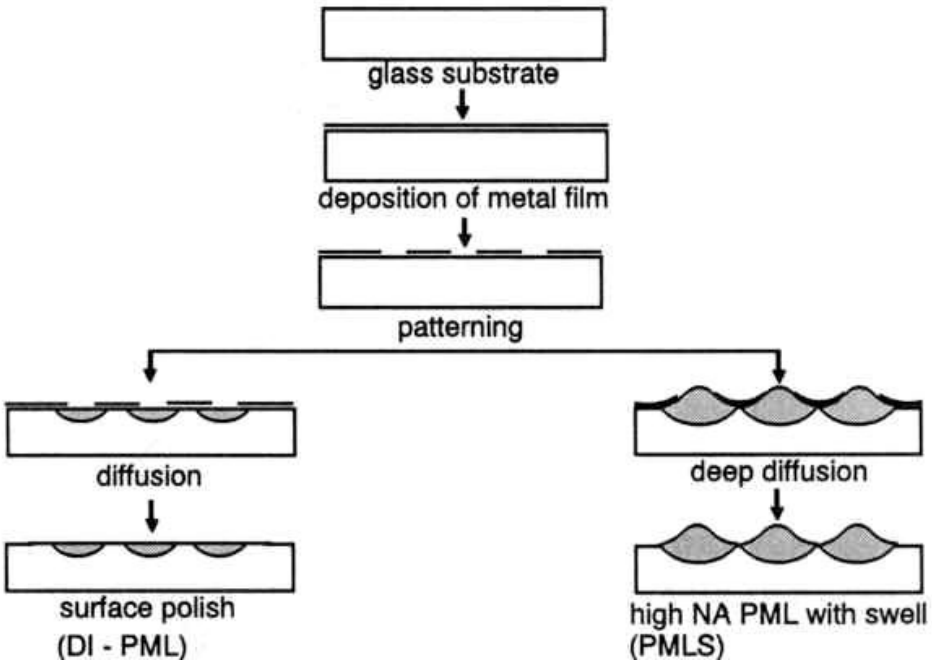
glass substrate
deposition of metal film
patterning
diffusion
surface polish
(DI - PML)
deep diffusion
high NA PML with swell
(PMLS)

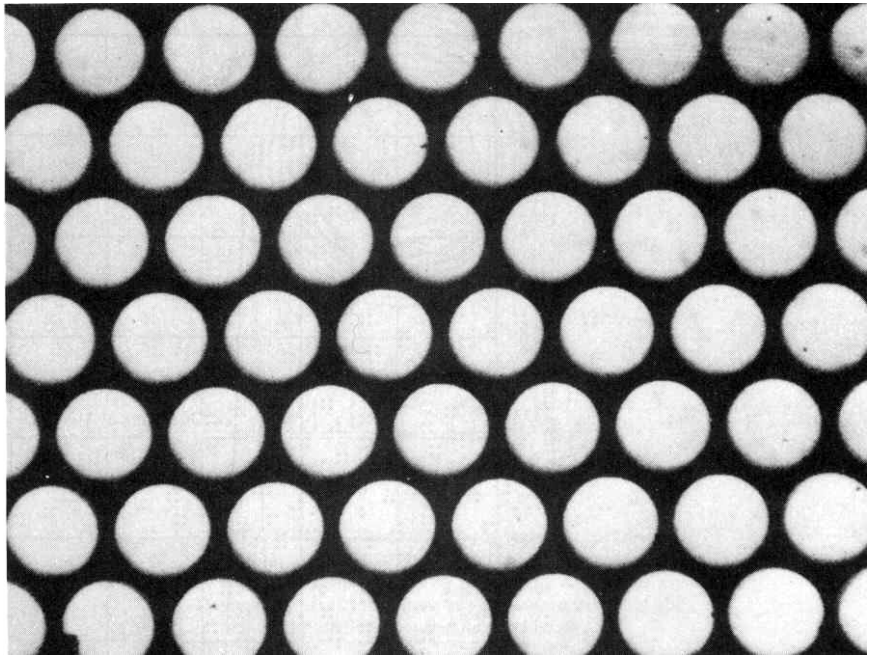

Microlens (II)

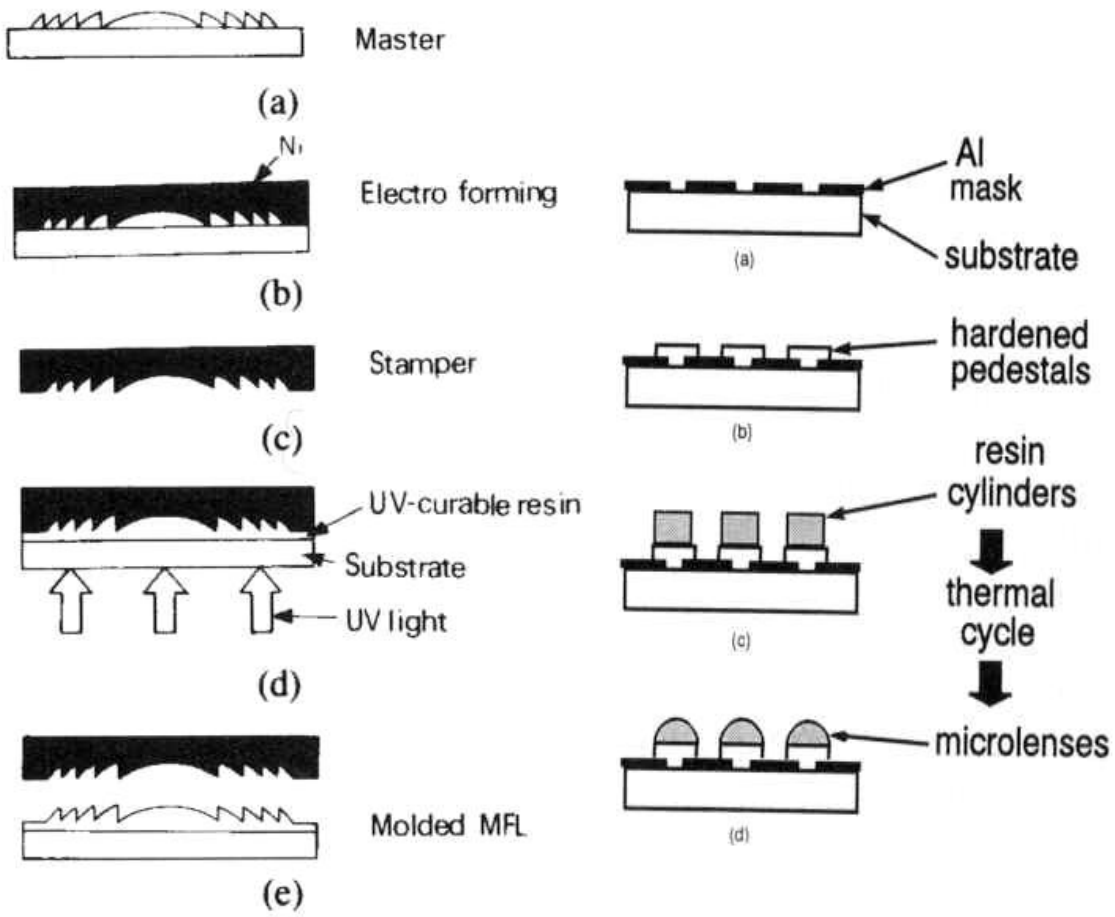

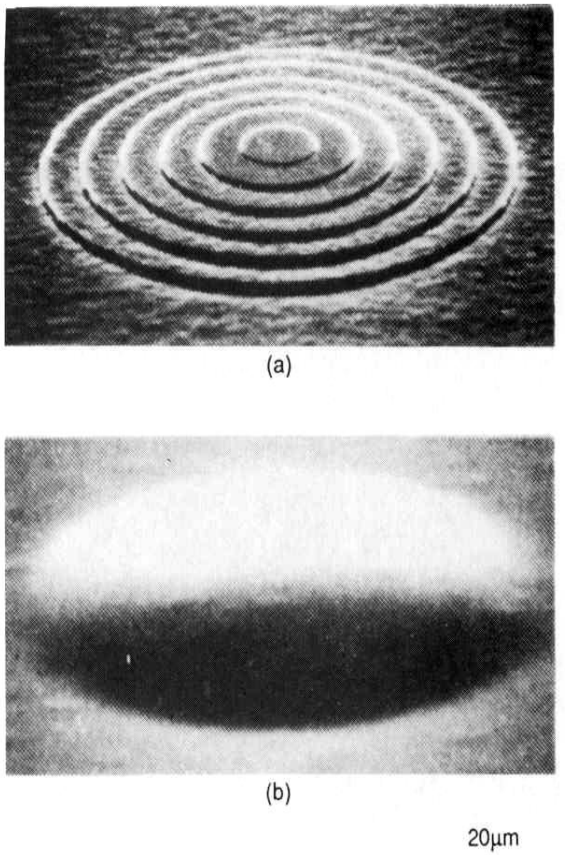

Microlens (III)

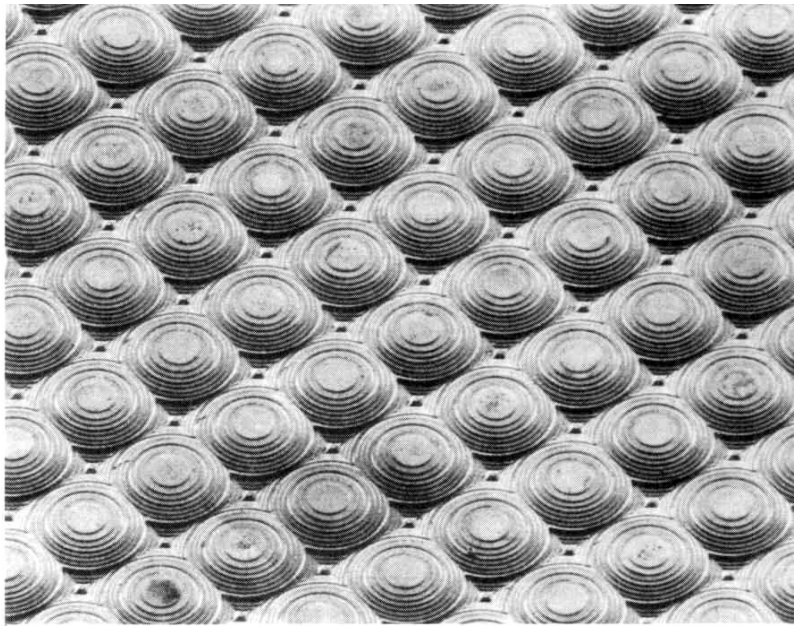

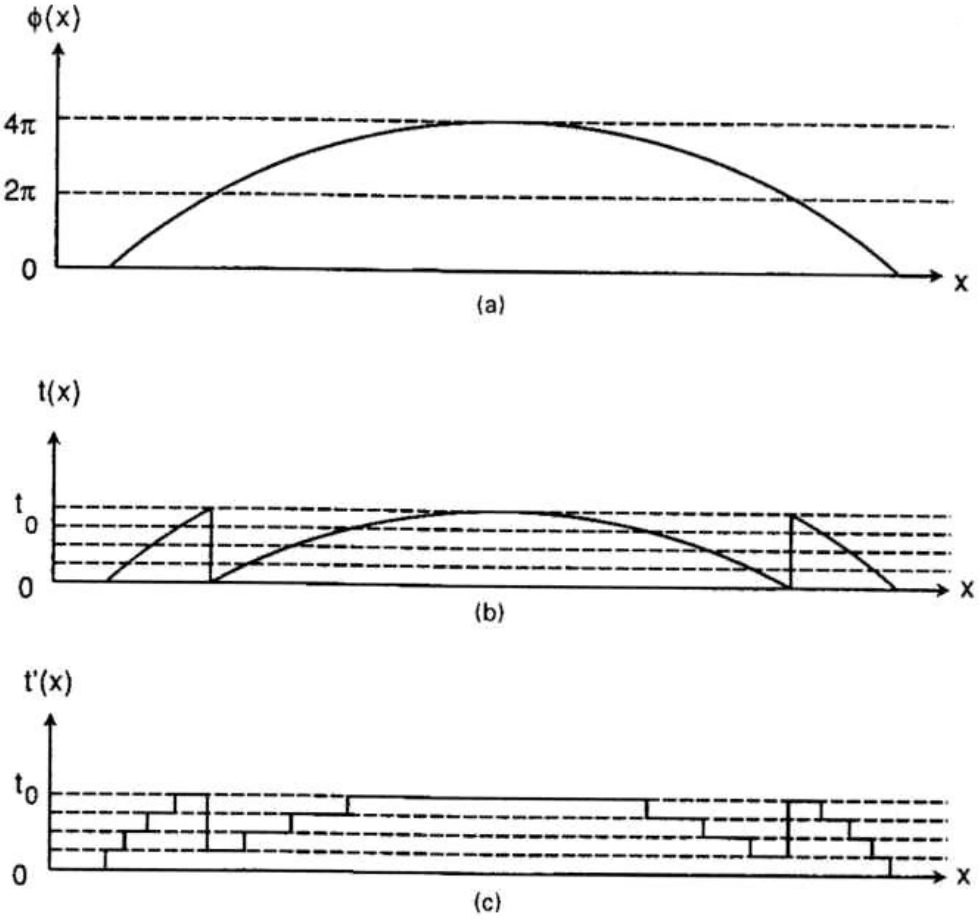

Wavefront Sensing

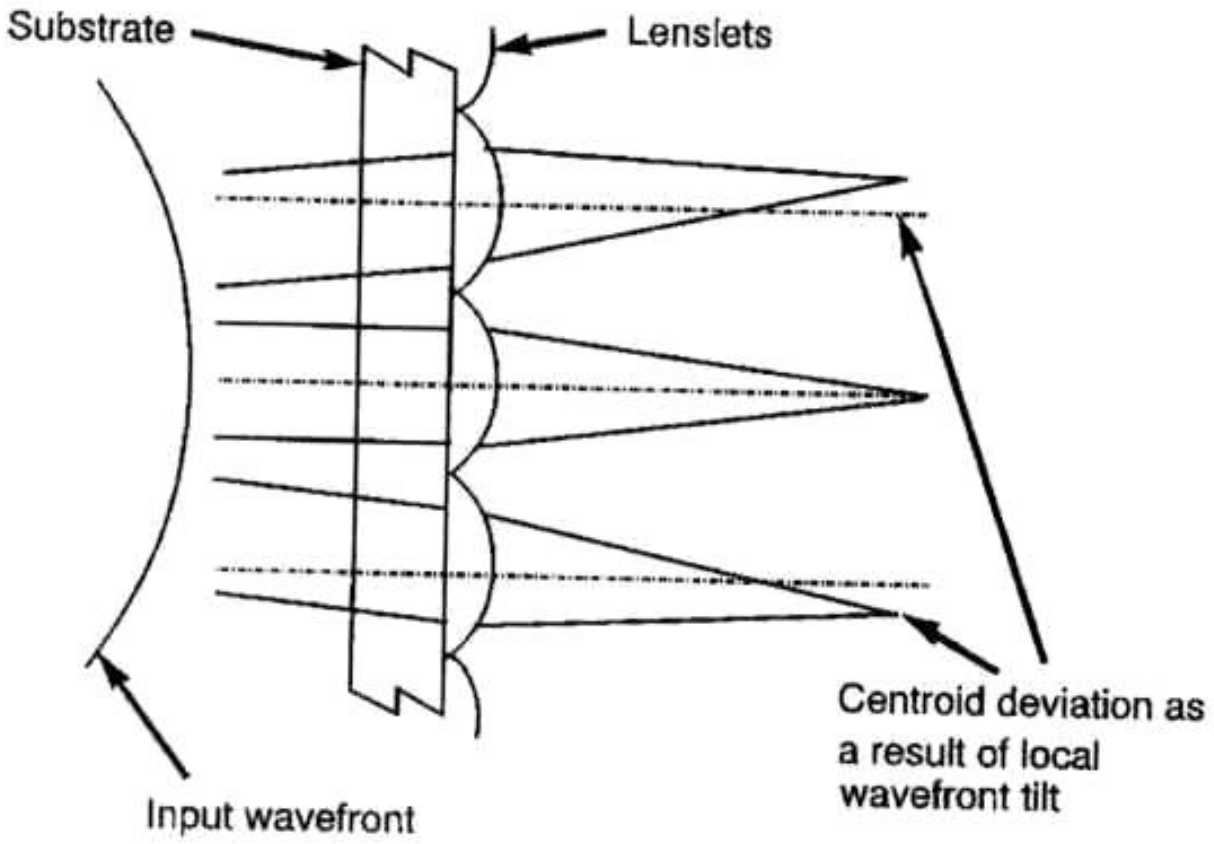

Microlens Array

- Micro-sized convex lens array
- Optical switching device for optical communication system
- Focusing device for optical data storage
- 3-D display component for super-multi view
- Various application for photonic devices

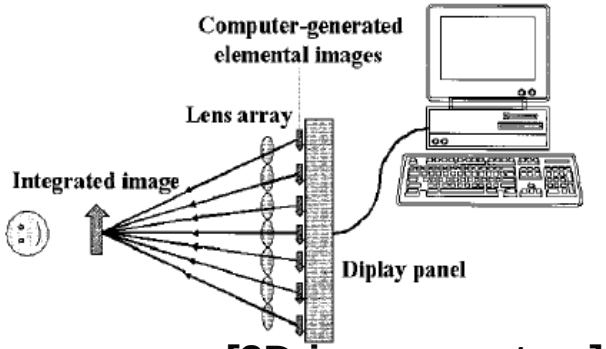

[3D-image system]

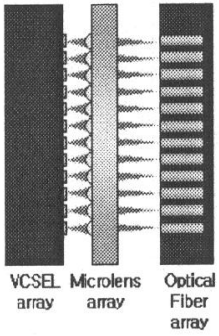

[Optical communication]

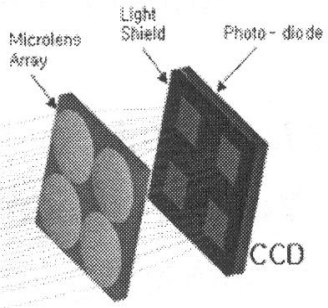

[Display/imager]

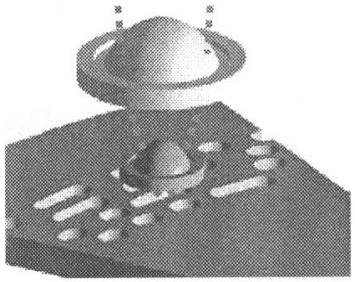

[Optical data storage]

Liquid Crystal Microlenses

- Patterned electrode type
- Surface-relief structure type
- FLC microlens using surface relief
- Input polarization dependence

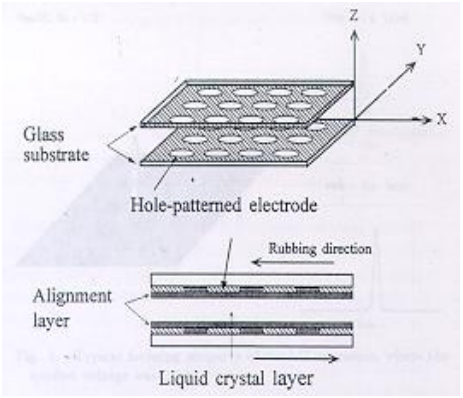

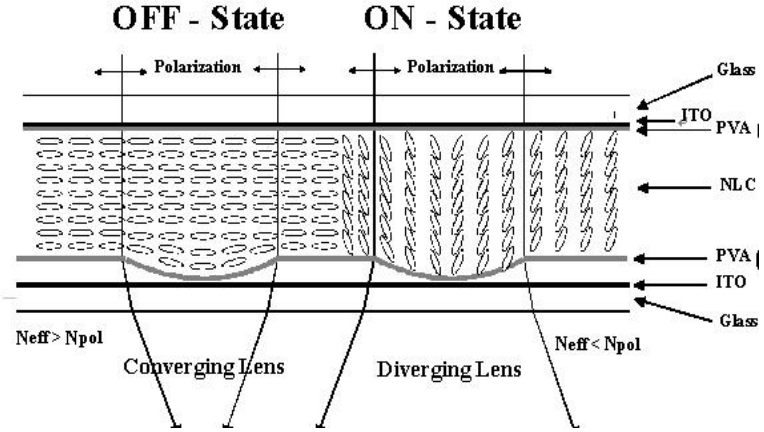

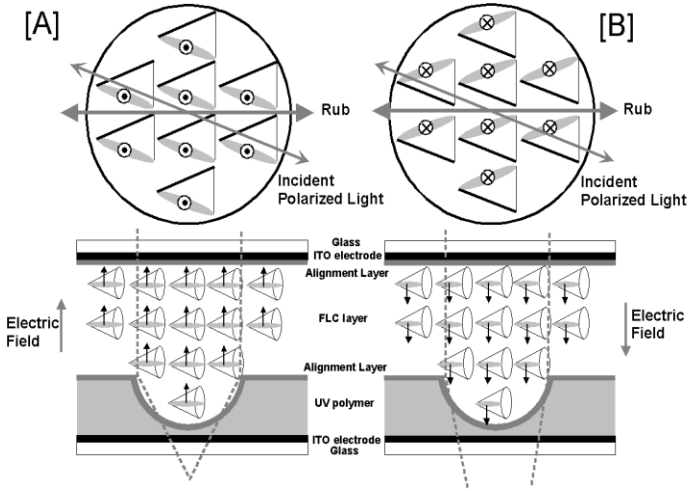

• ***In practical applications,***

Independence of Input Polarization is needed !!

Lord Rayleigh

Never say 'Never'!

J. W. Strutt

(1842-1919)

"…If it were possible to introduce at every part of the aperture of the grating an arbitrary retardation, all the light might be concentrated in any desired spectrum. By supposing the retardation to vary uniformly and continuously we fall upon the case of an ordinary prism; but there is then no diffraction spectrum in the usual sense. To obtain such it would be necessary that the retardation should gradually alter by a wave-length in passing over any element of the grating, and then fall back to its previous value, thus springing suddenly over a wave-length. It is not likely that such a result will ever be fully attained in practice; but the case is worth stating, in order to show that there is no theoretical limit to the concentration of light of assigned wave-length in one spectrum…"

Encylopaedia Britannica, 9th ed., Vol. 24, "Wave Theory of Light" (New York, Charles Schribner's Sons, 1888), p. 437

G. M. Morris

Tracor Flat-Panel ANVIS E-HUD*

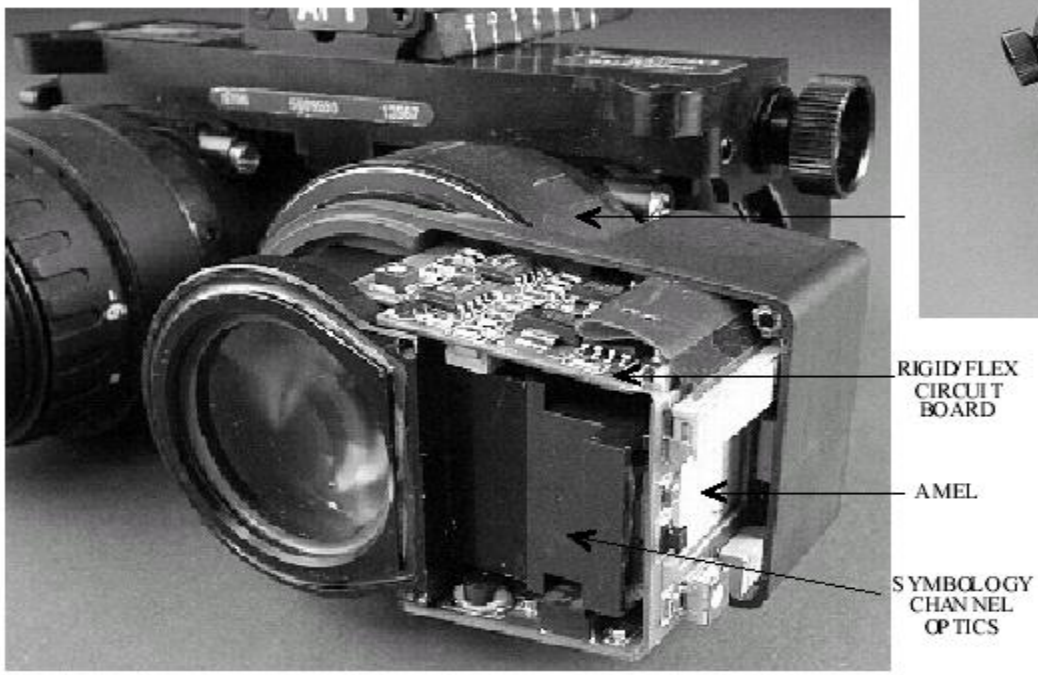

*E. F. Genaw, E. K. Nelson and K. F. Walsh, "Tracor Flat Panel ANVIS E-HUD," Proc. SPIE 3362 (1998).

Application Example

Rochester Photonics OEM Product

Pilot's Eye View

Applications
Flight lines
Factory Floors
Surgical Suites

G. M. Morris

Micropattering Using DOE and Femtosecond Laser

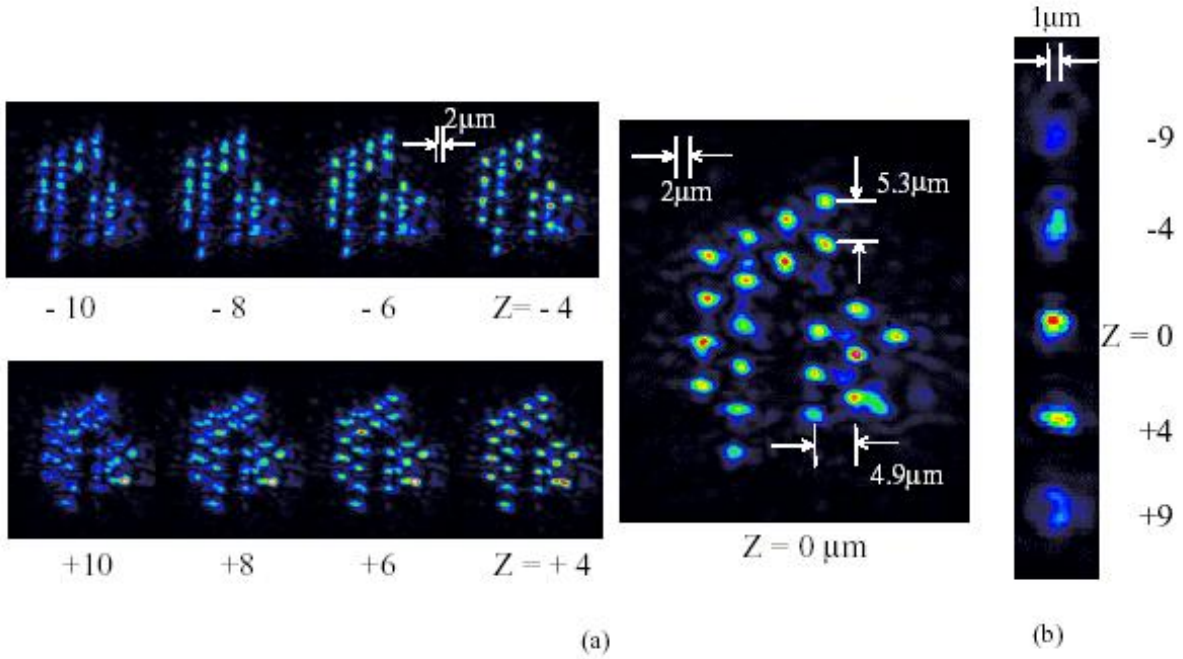

Fig. 4. Beam profile of focal point (a) with DOE and (b) without DOE.

Y. Kuroiwa *et al.*, Optics Express, vol. 12, no. 9, pp. 1908-1915, 2004.

DOE design problem

Basic layout of paraxial beam shaping system

Input field

$$W(x_1, y_1) = A(\Phi(x_1, y_1))\exp(j\Phi(x_1, y_1))$$

Output field

$$F(x_2, y_2) = \int_{-\infty}^{\infty}\int_{-\infty}^{\infty} h(x_2, y_2, x_1, y_1) W(x_1, y_1)\, dx_1 dy_1,$$

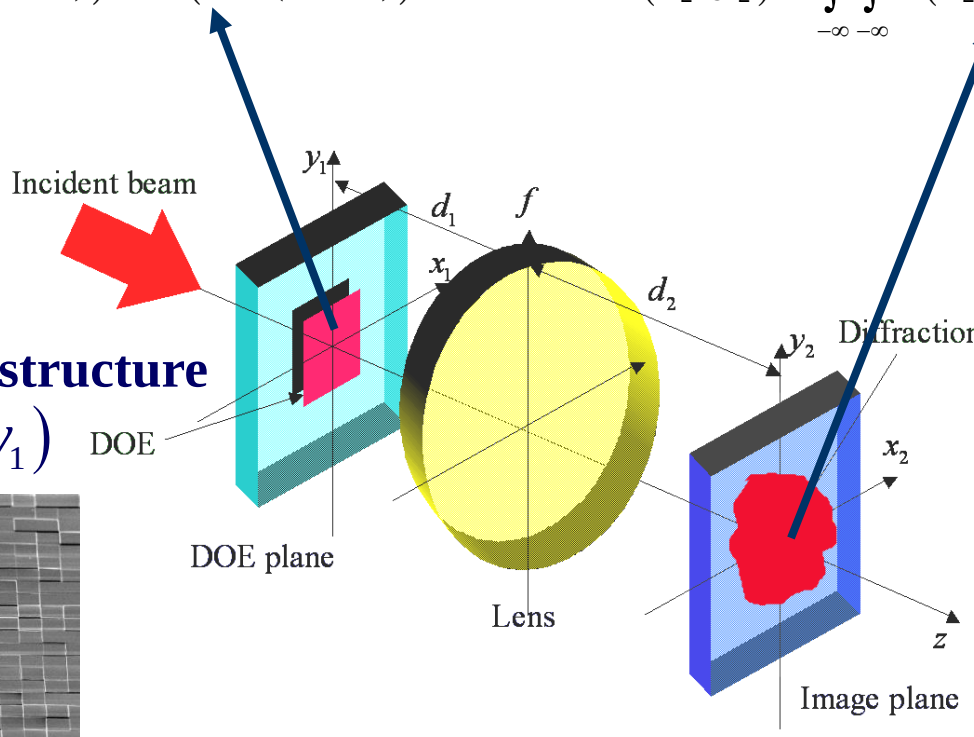

Surface relief structure of DOE $\Phi(x_1, y_1)$

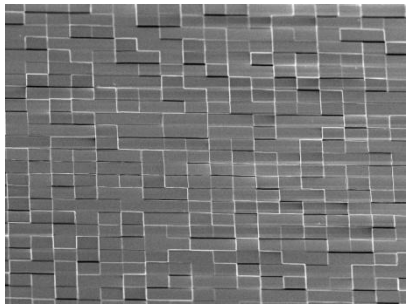

Diffraction image $F(x_2, y_2)$

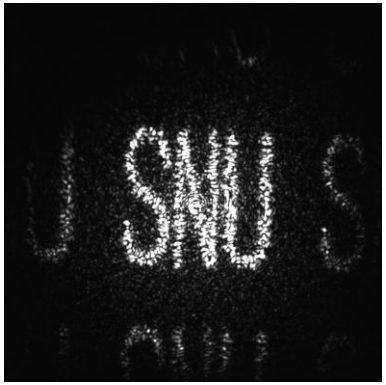

Nonlinear optimization methods for DOE design

- **Minimization scheme**

  Find $\Phi(x_1, y_1)$ for minimizing $E = \left\| I - \left| F(x_2, y_2) \right|^2 \right\|_{L_2}$

- **Iterative methods**
  - Iterative Fourier transform algorithm (IFTA)
  - Nonlinear conjugate gradient method (NCGM)

- **Stochastic methods**
  - Simulated annealing method (SA)
  - Genetic algorithm (GA)

- **Hybrid method**
  - SA or GA + IFTA or NCGM

Iterative Fourier transform algorithm (IFTA) for DOE design

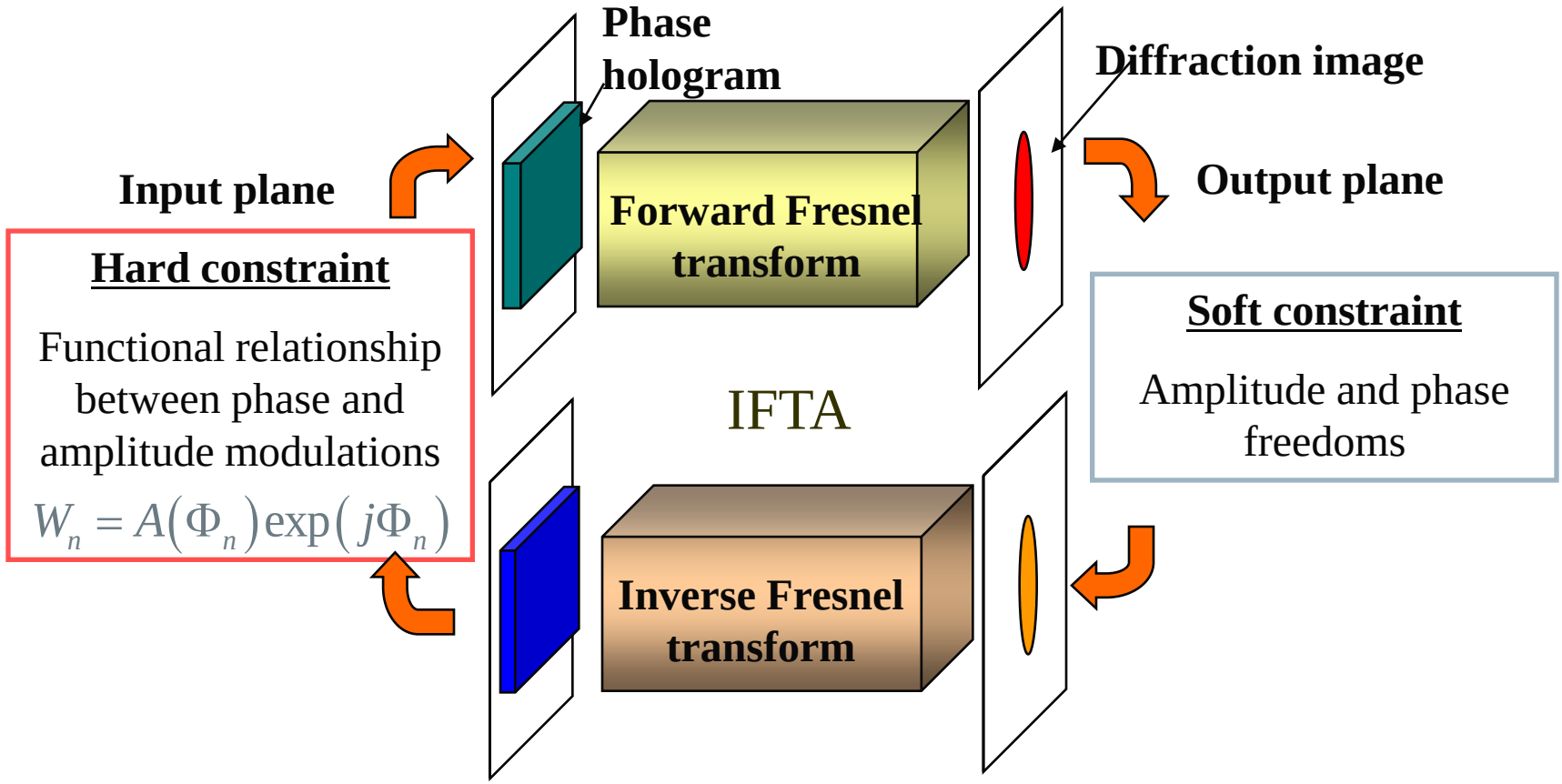

Existence of the analytic expression of the inverse Fresnel transform is the key of IFTA.

Regularization technique for obtaining the optimal trade-off between diffraction efficiency and uniformity

- IFTA scheme with Tikhonov regularization scheme (adaptive regularization parameter distribution)

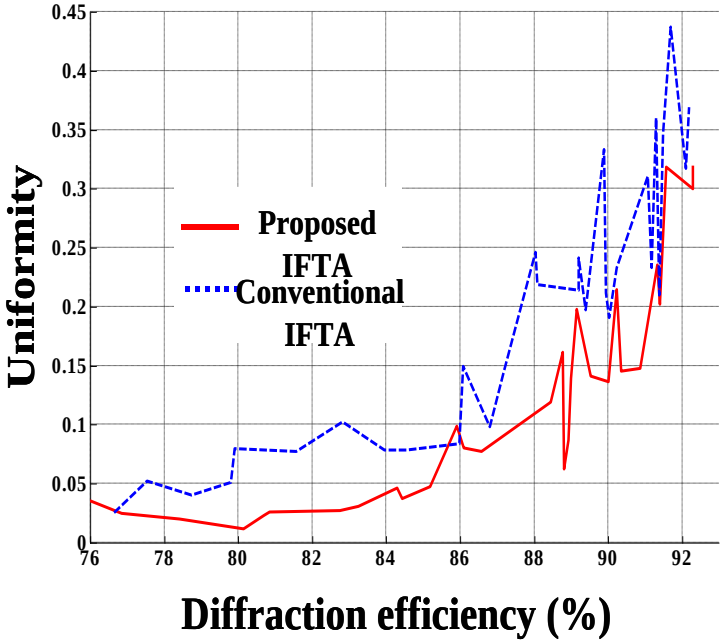

Proposed design

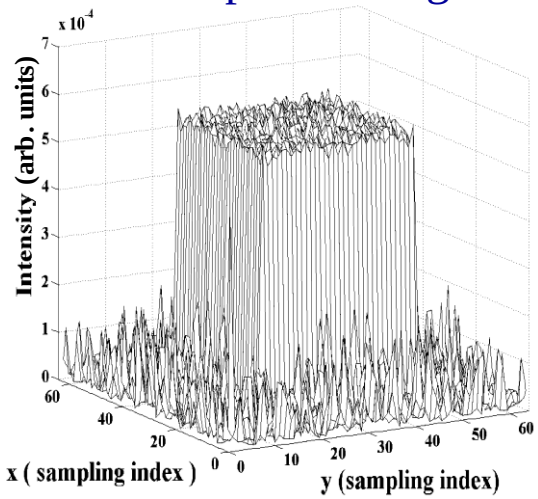

Diffraction efficiency=84.7%
Uniformity=0.0365

Conventional design

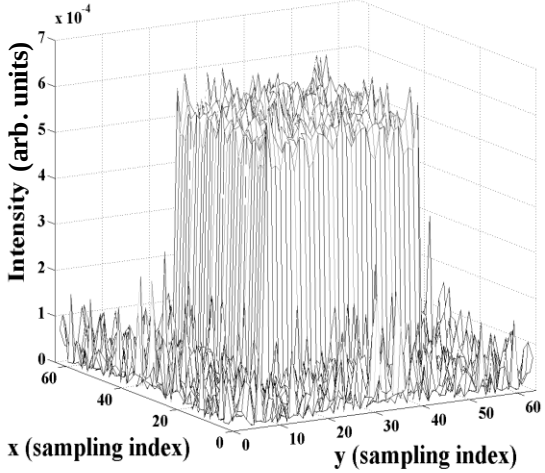

Diffraction efficiency=84.5%
Uniformity=0.0746

H. Kim, B. Yang, and B. Lee, Journal of the Optical Society of America A, vol. 21, p. 2353, 2004.

H. Kim and B. Lee, Japanese Journal of Applied Physics, vol. 43, no. 6A, p. L702, 2004.

Hybrid scheme of IFTA and GA for optimal IFTA convergence

Micro genetic algorithm

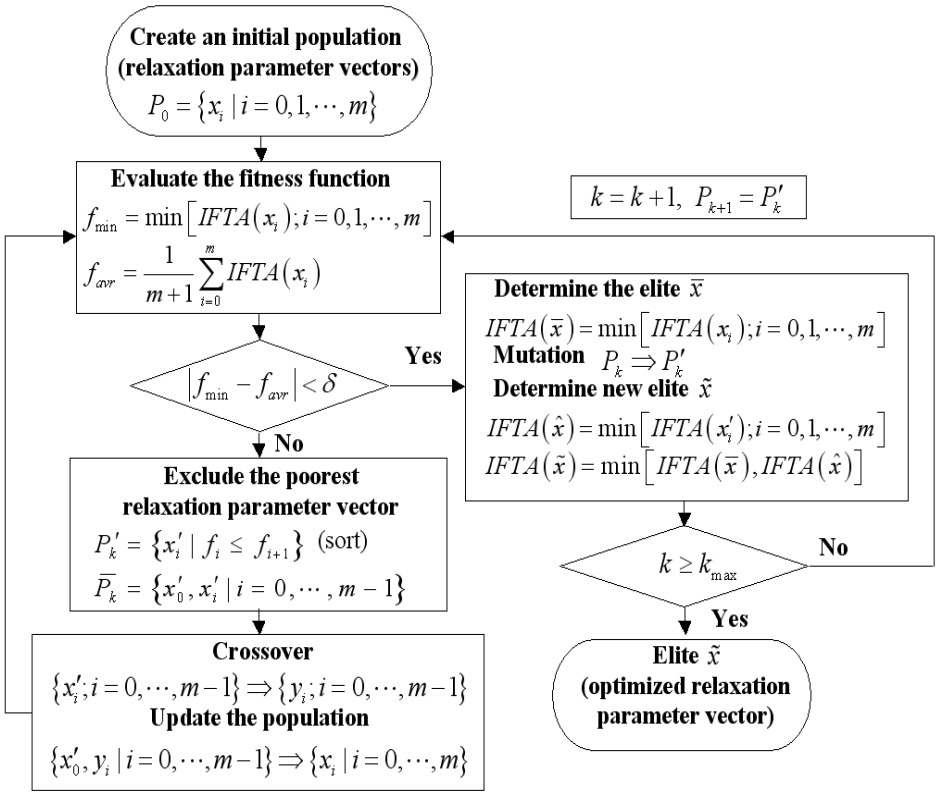

IFTA

$$F_n \leftarrow \begin{cases} \lambda_n F_0 \exp(j\psi_n) + \left(1 - \lambda_n - \frac{2\lambda_n}{\pi}\tan^{-1}\left[\frac{|F_n(x,y)| - F_0(x,y)}{F_0(x,y)}\right]\right) F_n & \text{for } (x,y) \in S \\ +\lambda_n \alpha_D \nabla^2 |F_n| \exp(i\psi_n) & \\ F_n & \text{for } (x,y) \notin S \end{cases}$$

Micro genetic algorithm + IFTA

- Micro genetic algorithm finds the optimal relaxation parameter vector of the imbedded IFTA scheme.
- IFTA shows non-monotonic optimal convergence.

H. Kim and B. Lee, Optics Letters, vol. 30, p. 296, 2005.

Non-monotonic optimal convergence of IFTA

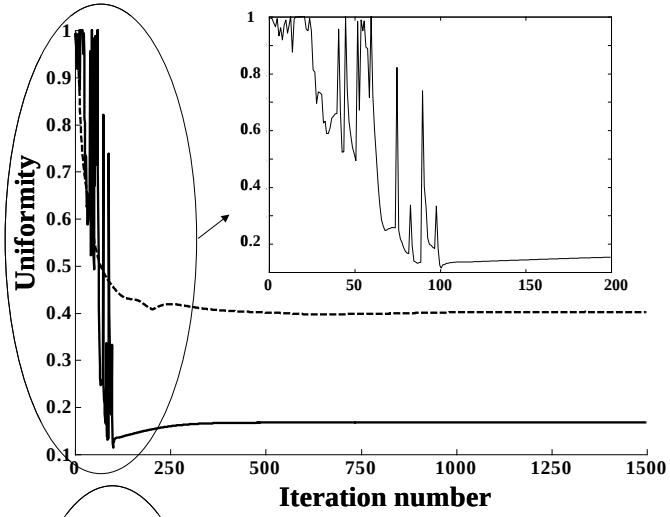

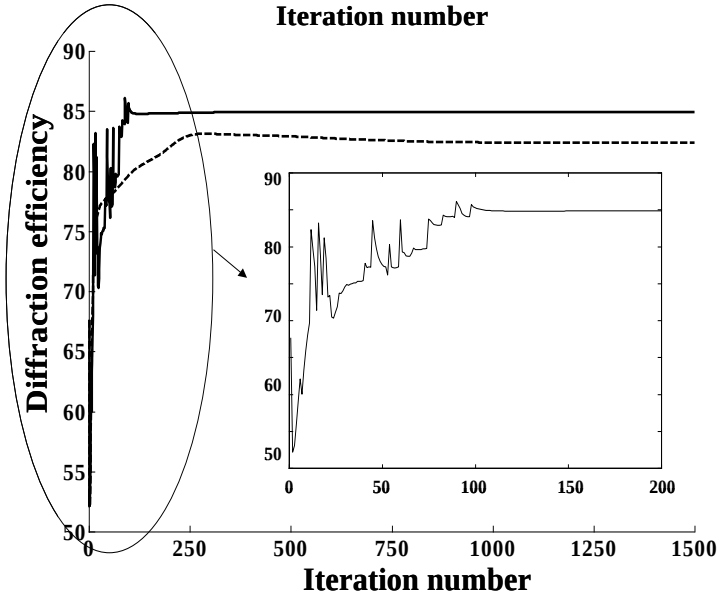

Proposed design

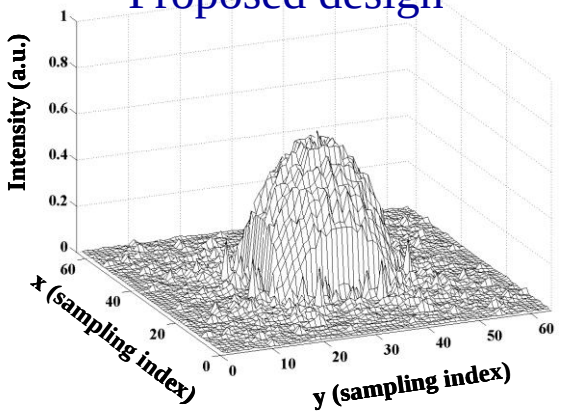

Diffraction efficiency=85.7%
Uniformity=0.113

Conventional design

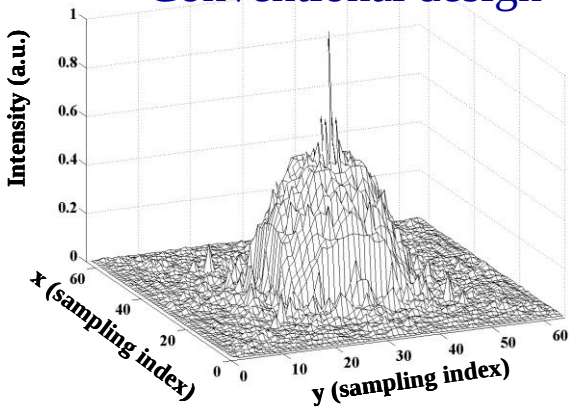

Diffraction efficiency=82.4%
Uniformity=0.401

Speckle reducing problem in DOE design

Obtained diffraction image

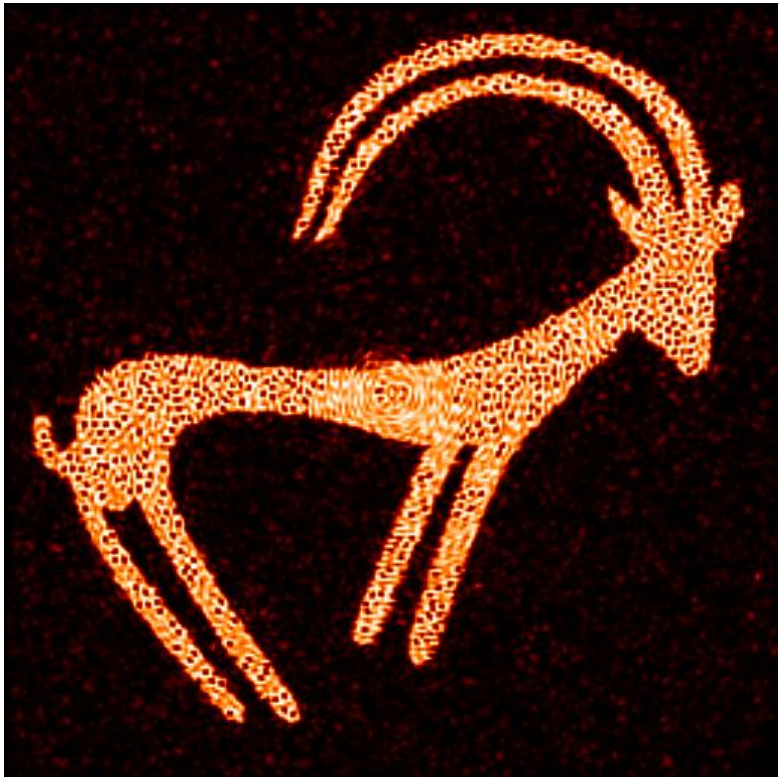

Phase profile of conventional DOE

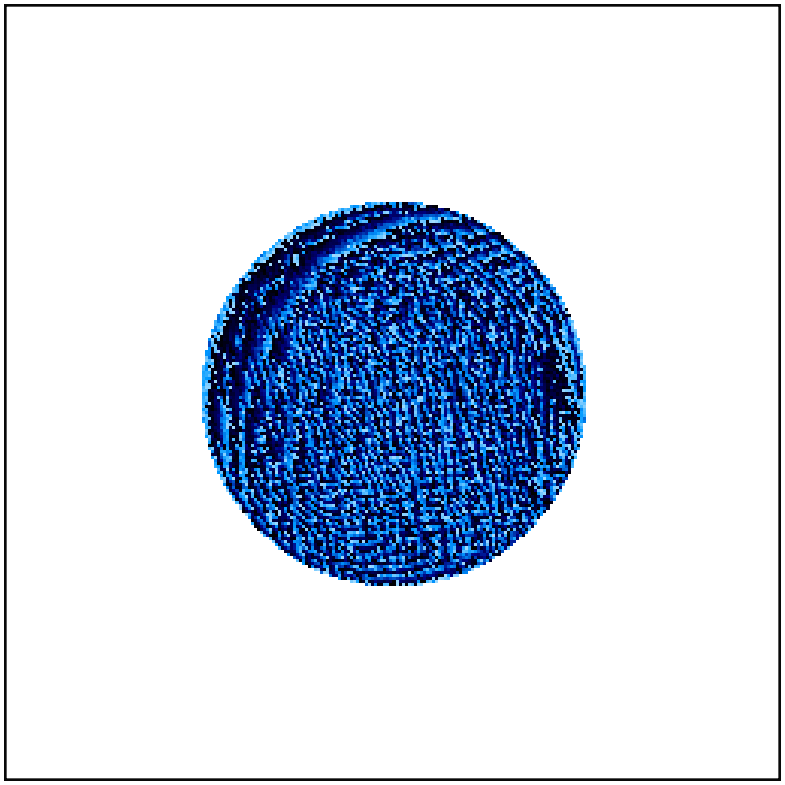

Optical vortices appear in the diffraction image generated by a conventional DOE

Boundary modulated DOE design

Obtained diffraction image

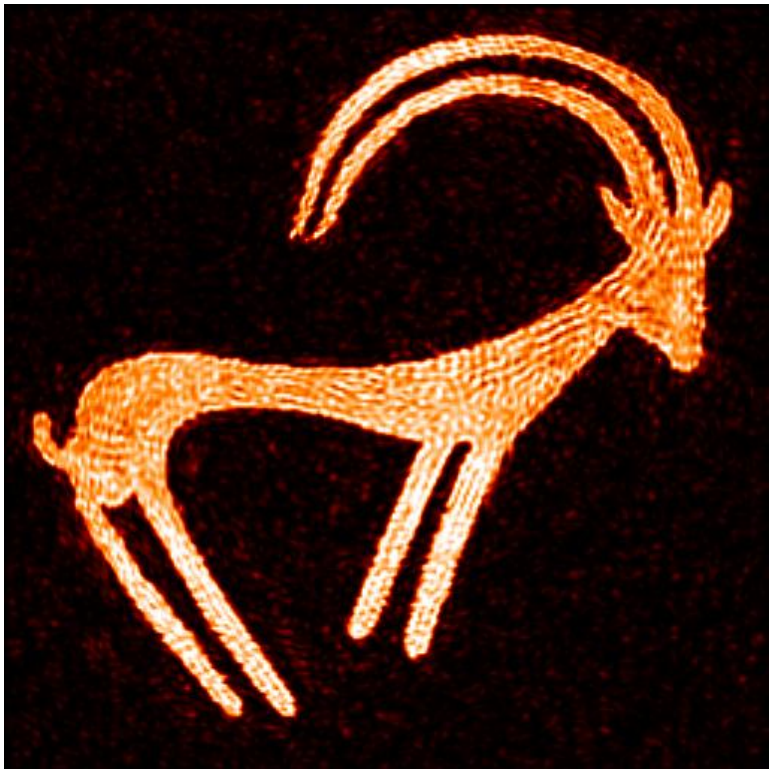

Phase profile of the proposed DOE

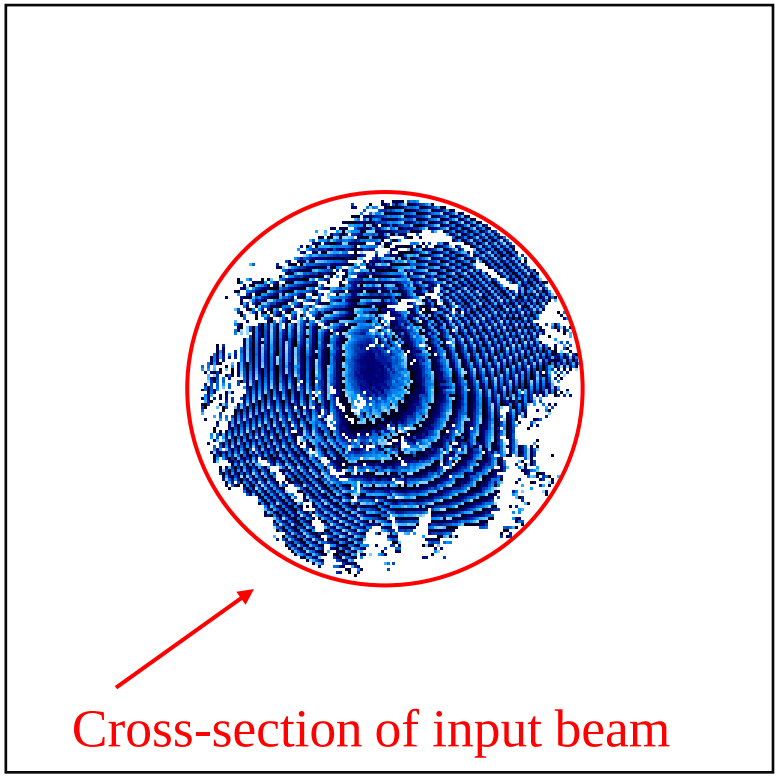

Optical vortices are eliminated in the diffraction image generated by the proposed boundary modulated DOE

H. Kim and B. Lee, Japanese Journal of Applied Physics, vol. 43, no. 12A, p. L1530, 2004.

Accurate modeling of the transmittance functions of DOEs

The transmittance function of a multilevel DOE is calculated considering internal multiple reflections inside the DOE structure.

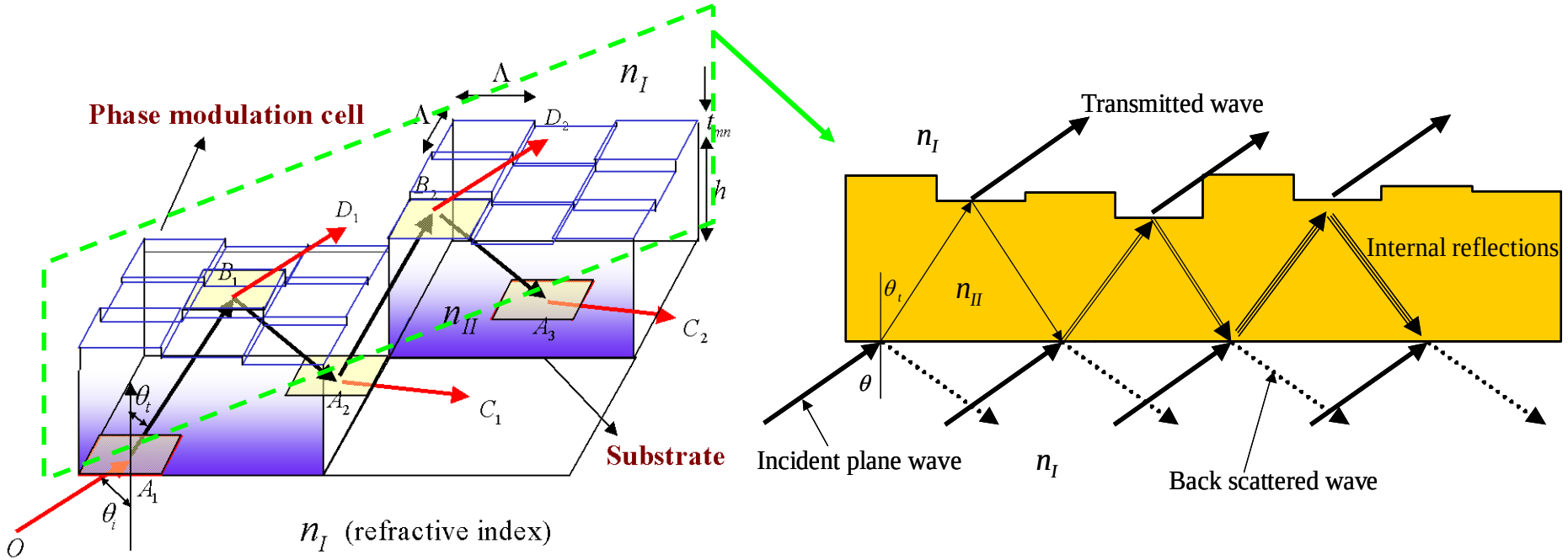

H. Kim and B. Lee, Optical Engineering, vol. 43, no. 11, p. 2671, 2004.

Comparison of the proposed transmittance function with the conventional transmittance function

Conventional design

Proposed design without phase errors

Normal incidence

Phase error

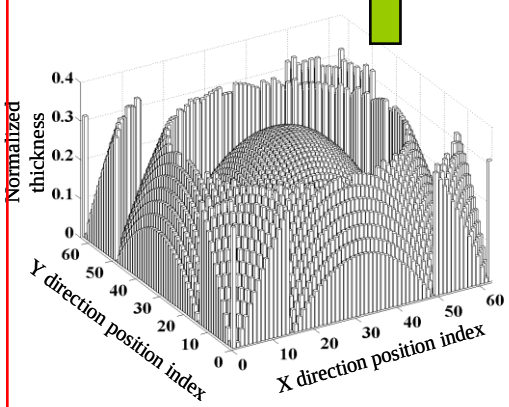

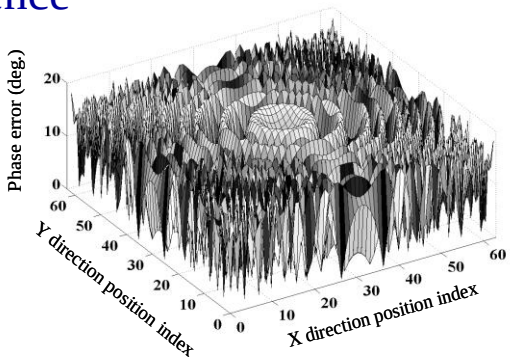

Refractive index=3.4

Oblique incidence

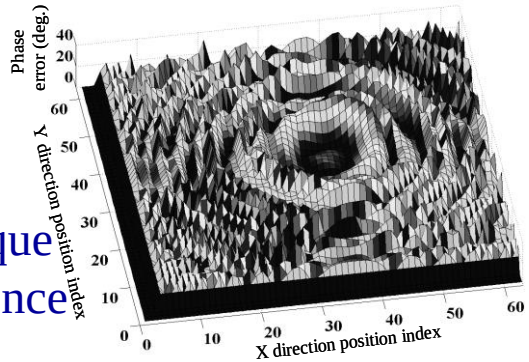

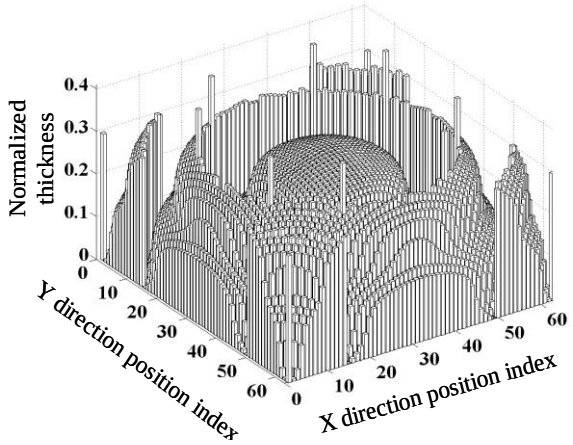

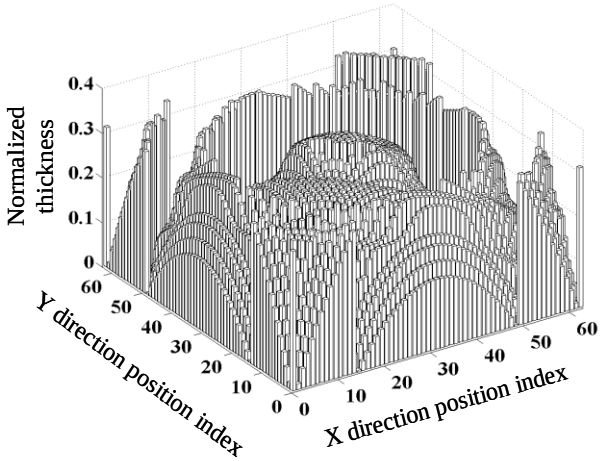

Speckle reduction for laser display

- **Laser display system and speckle problem**
  - The speckle patterns impair the image quality (strong deblurring of the color edges)
  - Low transmission efficiency and deterioration of the laser beam quality
  - Coherence degradation of the light source, diffuser, digital image processing of signals

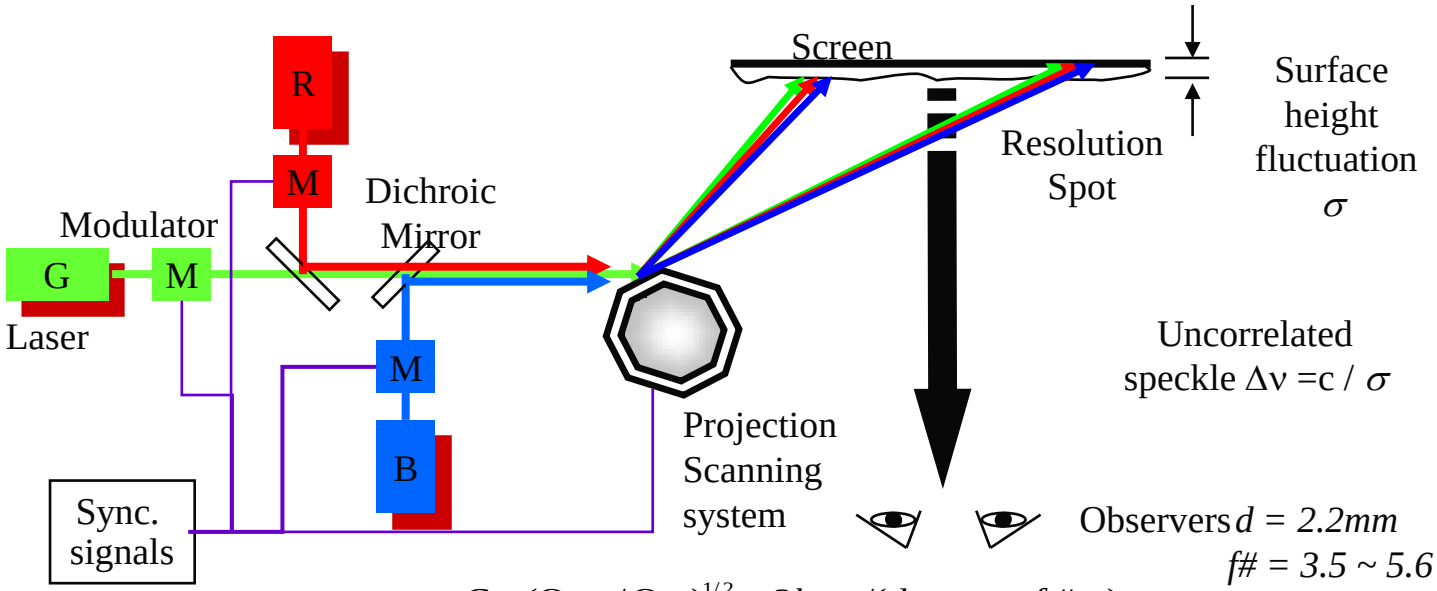

$$C = (\Omega_{proj} / \Omega_{\det})^{1/2} = 2h_{pixel} / (d_{pupil\_size} \cdot f\#_{eye})$$

Speckle reduction for laser display

- **Speckle configuration**

  - Speckle contrast ratio: "Severe" speckle is associated with contrast measurements of $C > 0.30$

$$C = \frac{\sqrt{\langle I_i^2 \rangle - \langle I_i \rangle^2}}{\langle I_i \rangle} = \frac{\sigma}{\mu}$$

where, $\langle I_i \rangle$: intensity of the i^{th} pixel of a CCD
σ : standard deviation, μ : mean value

✓ Comparison of speckle degradation methods

Component	Speckle contrast	Speckle reduction(%)	Insertion loss(%)
Stationary diffractive diffuser	**0.312**	**3.4**	**5**
Refractive lens array(6×8)	**0.309**	**4.3**	**14**
Fiber, 2m	**0.262**	**18.9**	**20**
Vibrated fiber	**0.057**	**82.4**	**20**
Vibrated diffractive diffuser	**0.048**	**85.1**	**5**
Vibrated projection screen	**0.034**	**89.5**	**0**
All vibrated components & lens arrays	**0.009**	**97.2**	**35**

IEEE LEOS '99, pp.354-355.

Speckle reduction using DOEs

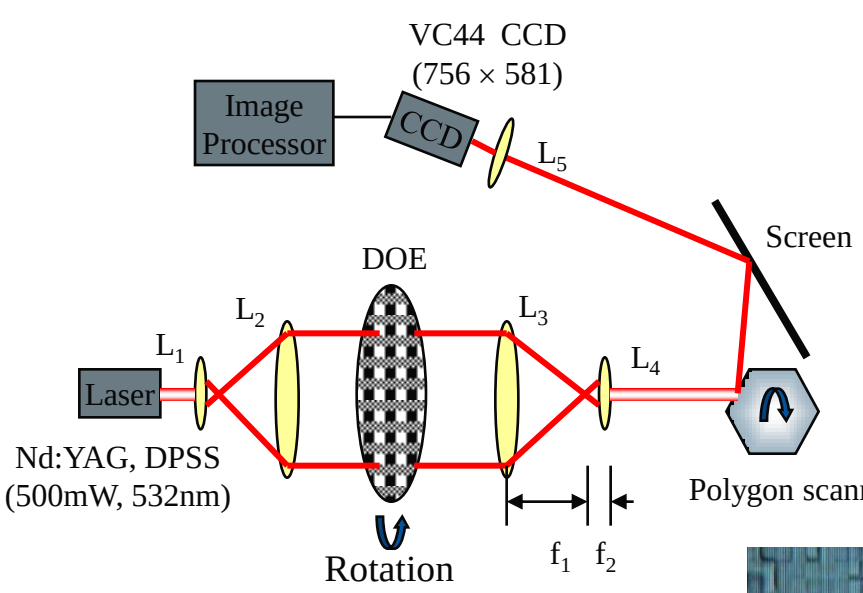

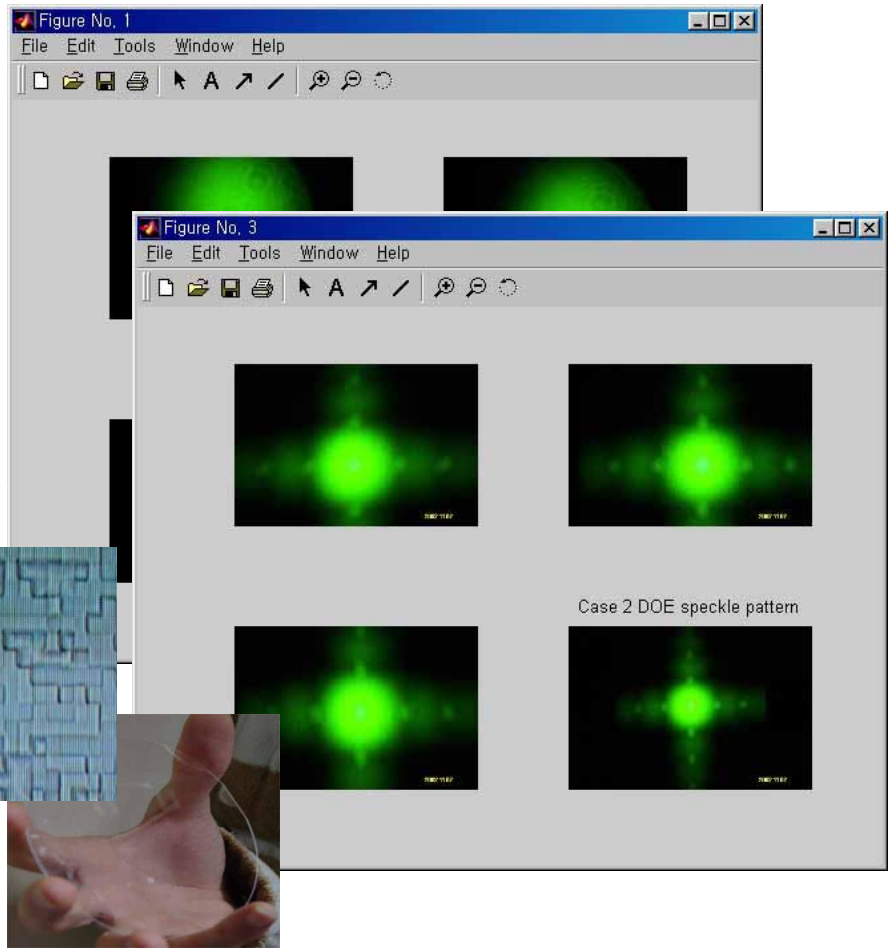

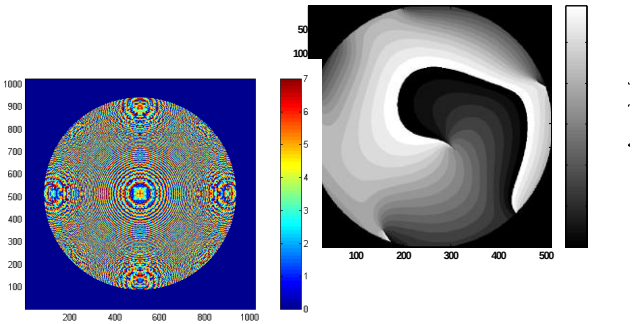

Speckle reduction using DOEs

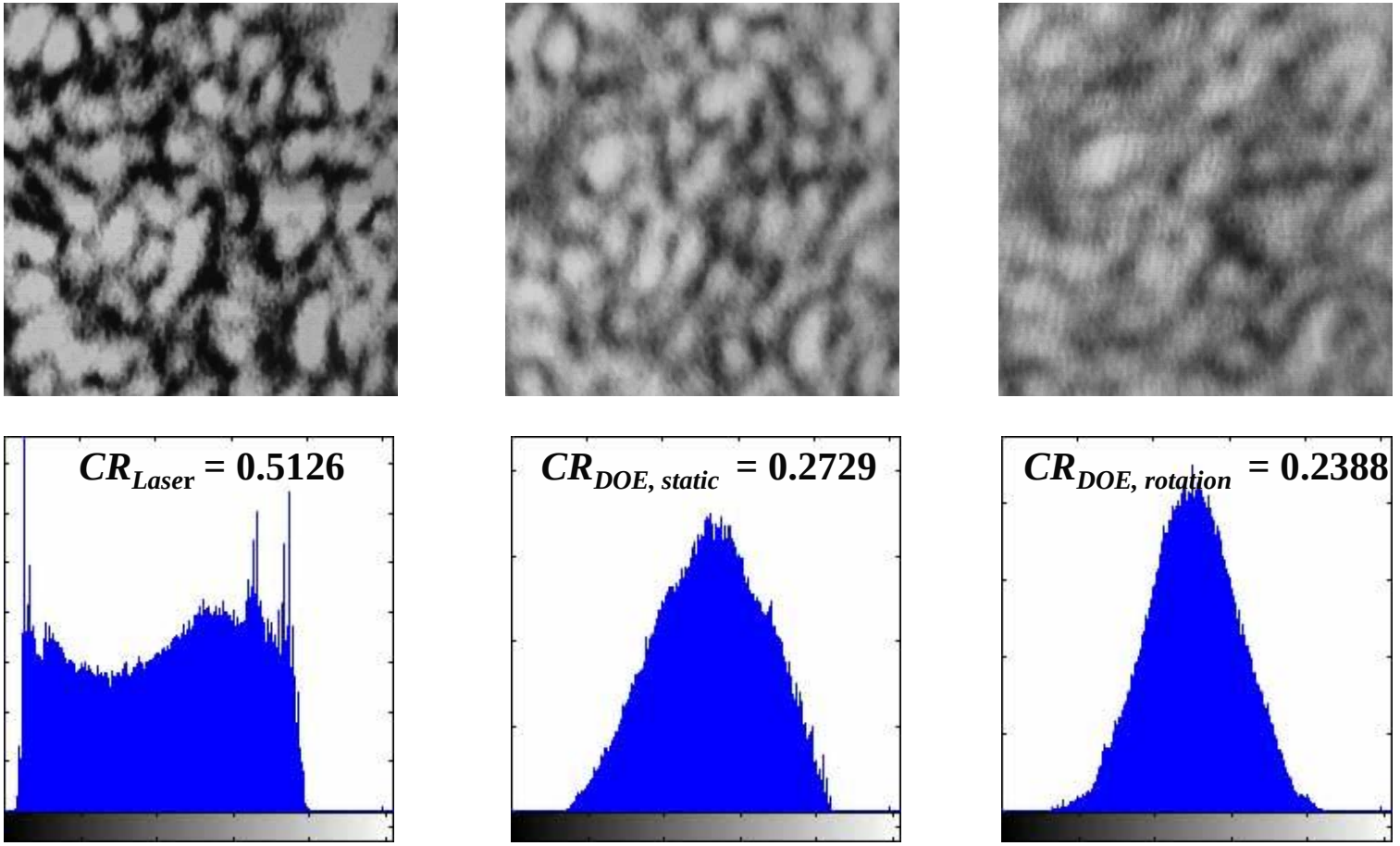

Speckle pattern and its histogram of Nd:YAG laser source, (static DOE, and rotating DOE (5rps).

DOE design for non-invertible Fresnel diffraction integral

IFTA is not applicable for the design of DOEs for making diffraction images on an arbitrarily curved surface.

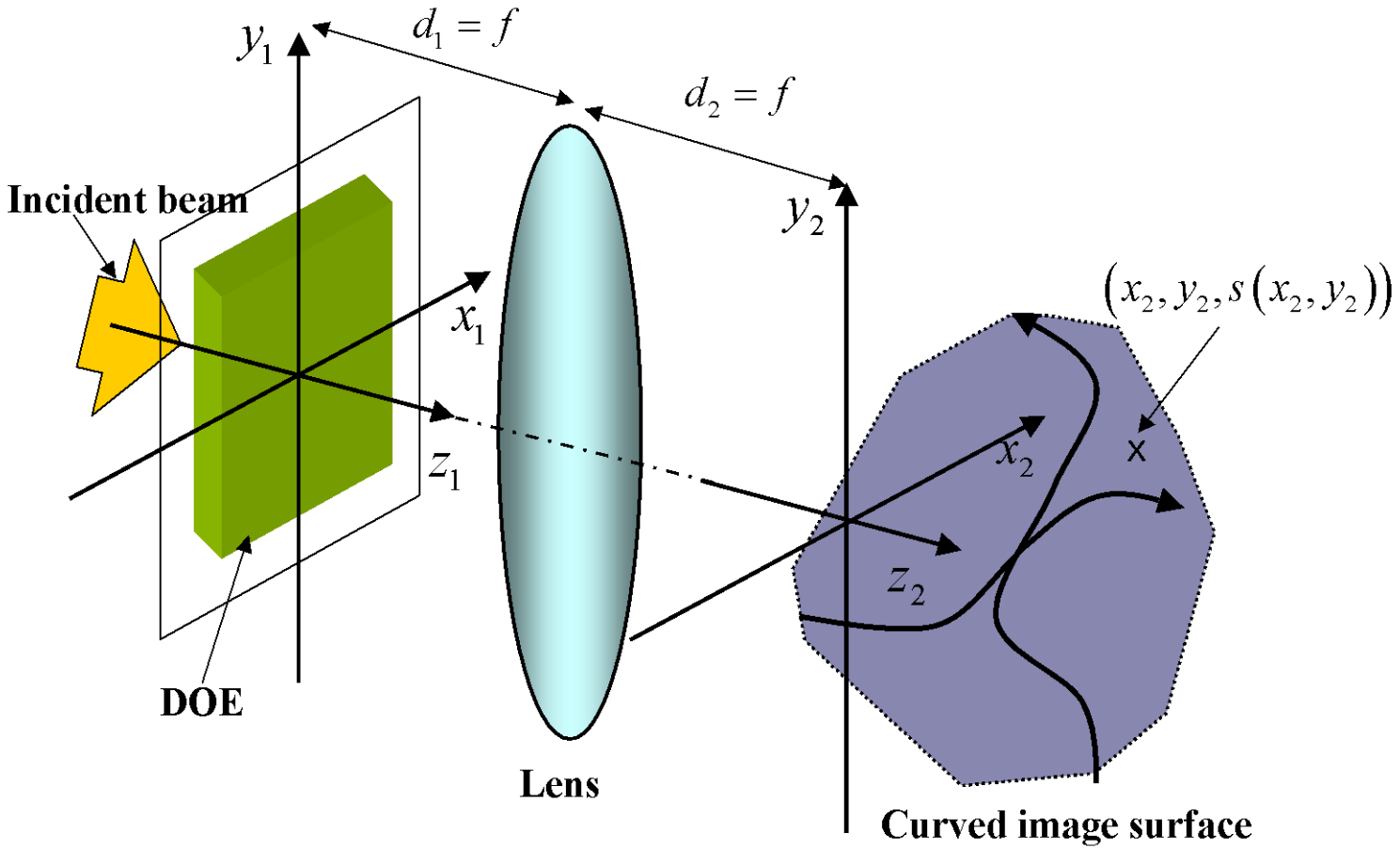

Nonlinear conjugate gradient method

Objective function

$$E(\mathbf{\Phi}) = \sum_{m}^{N^2} \left[\beta(m) \left| \sum_{n}^{N^2} G_{mn} A(\phi_n) \exp(j\phi_n) \right| - I_m \right]^2$$

I_m Target image

$\beta(m)$ Weight distribution

Flow chart of NCGM

$$\mathbf{d}_0 = -\nabla E(\mathbf{\Phi}_0)$$

$$\tau_k \quad \textbf{for} \quad \min\left[E(\mathbf{\Phi}_{k+1}; \tau_k) \right]$$

$$\mathbf{\Phi}_{k+1} = \mathbf{\Phi}_k + \tau_k \mathbf{d}_k$$

Bracketing algorithm
Golden section line search

$$\beta_{k-1} = \frac{\left|\nabla E(\mathbf{\Phi}_k)\right|^2}{\left|\nabla E(\mathbf{\Phi}_{k-1})\right|^2}$$

$$\mathbf{d}_k = -\nabla E(\mathbf{\Phi}_k) + \beta_{k-1} \mathbf{d}_{k-1}$$

Fletcher-Reeves formula

$$k \rightarrow k+1$$

Design example

- **Amplitude function as a function of phase**

$$A(\phi) = c_0 + \sum_{h=3}^{7} c_h \left(\phi^h - (2\pi)^{h-1} \phi - 7/2 (2\pi)^{h-2} \left(\phi^2 - 2\pi\phi \right) \right) \quad \text{for } (x_2, y_2) \in \Gamma$$

$$A(0) = A(2\pi) \quad A'(0) = A'(2\pi)$$

- **Curved output surface (defocus surface)**

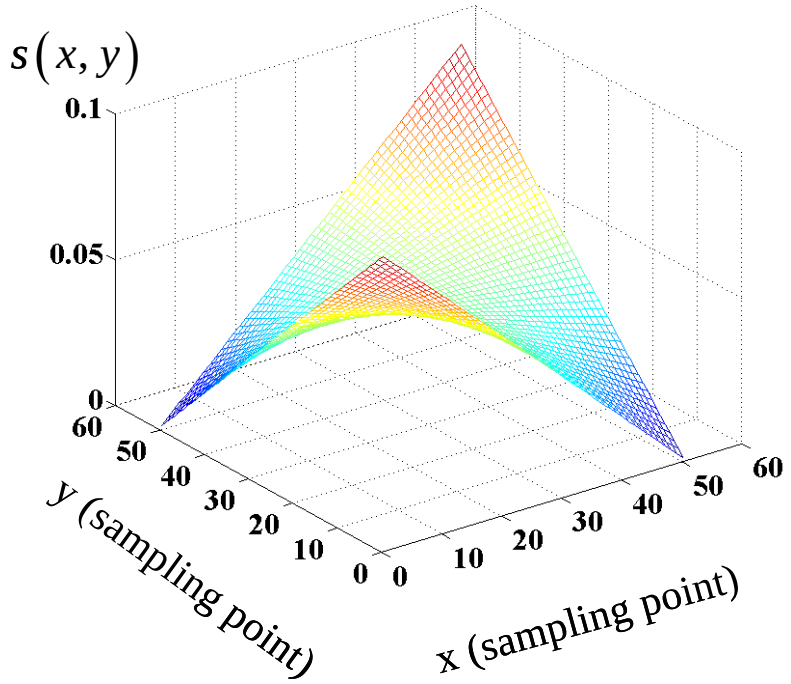

- **Target image**

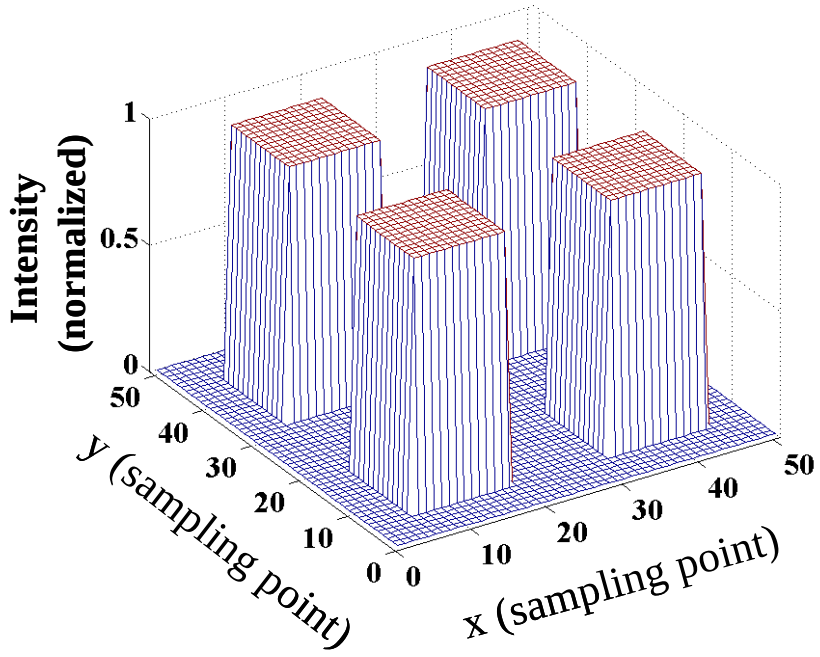

Diffraction simulation

DOE for curved surface

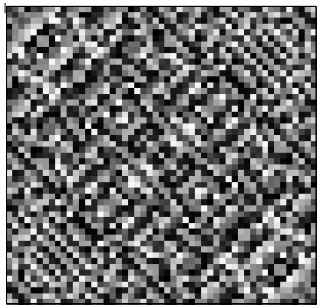

DOE for flat surface

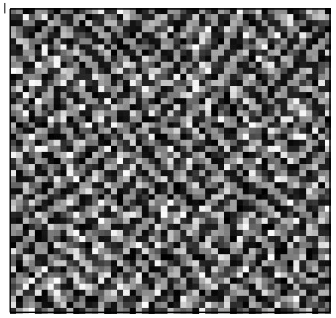

Field amplitude distribution on the curved output surface

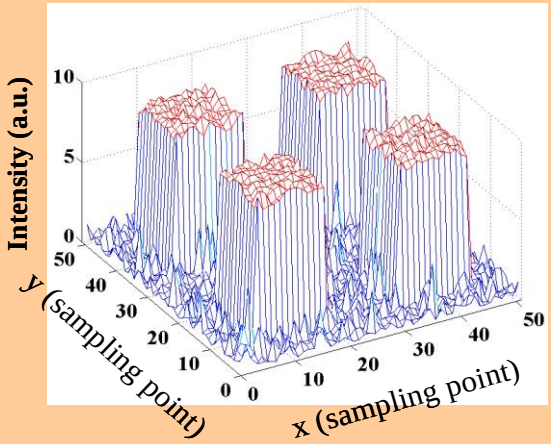

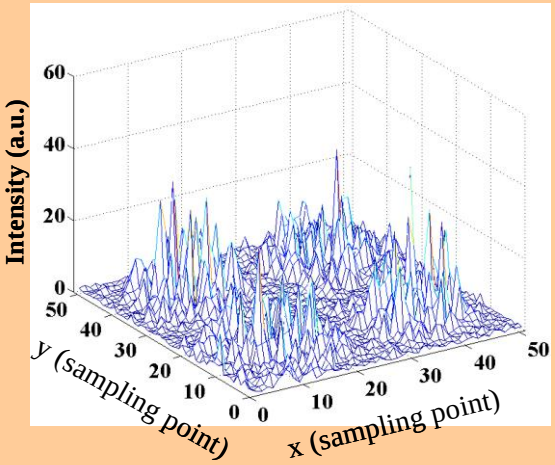

Field amplitude distribution on the flat plane (z_2=0)

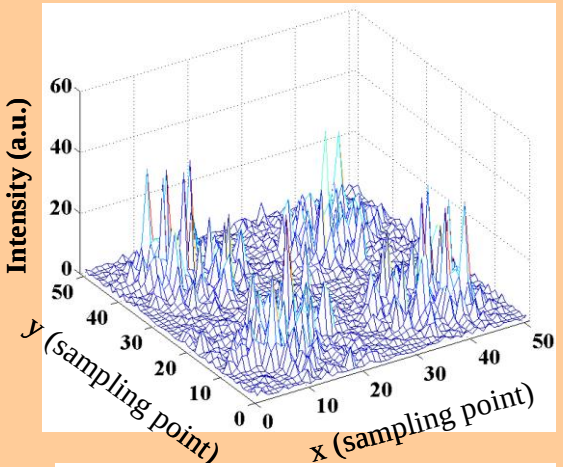

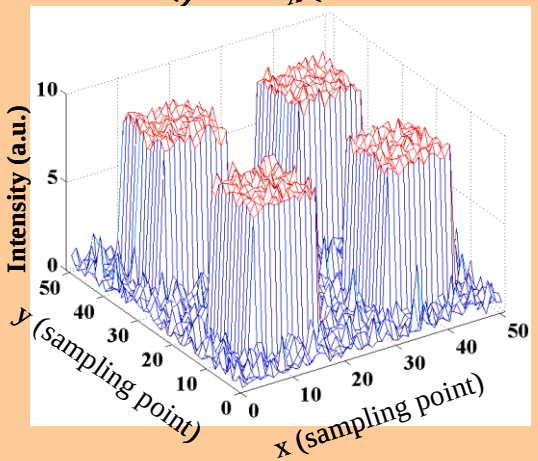

Electromagnetic analysis on subwavelength scale DOEs

Binary surface relief structure on a subwavelength scale can modulate both phase and amplitude of the incident optical field.

Fourier expansion of binary subwavelength scale grating

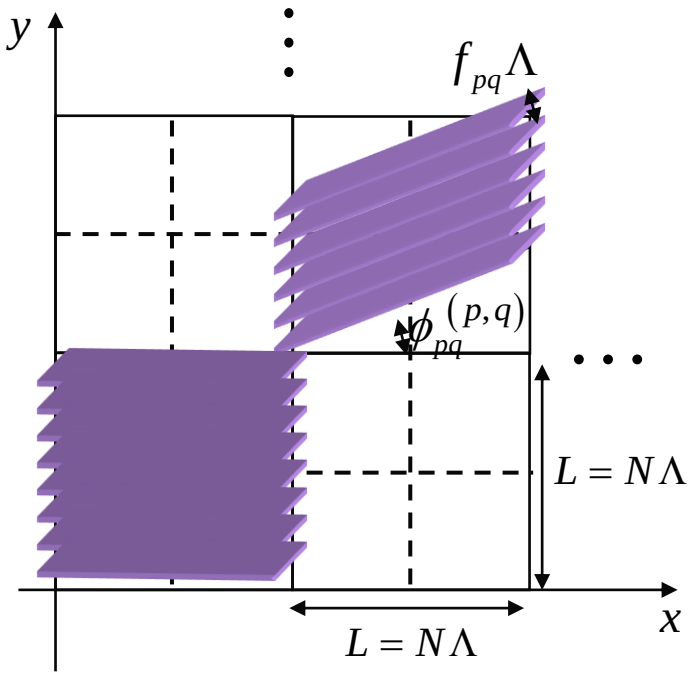

$$\varepsilon(x,y) = \sum_{m=-\infty}^{\infty}\sum_{n=-\infty}^{\infty} \varepsilon_{mn} \exp\left(j2\pi \left(\frac{m}{T_x}x + \frac{n}{T_y}y \right) \right)$$

$$\varepsilon_{mn} = \frac{1}{T_x T_y} \sum_{p=1}^{M}\sum_{q=1}^{M} [D_{mn}(p,q)\left(n_2^2 - n_1^2\right) f_{pq}$$

$$\times \sum_{k=-\infty}^{\infty} \operatorname{sinc}\left(k f_{pq}\right) \exp\left(-j\pi k \left(f_{pq} + L\left(\frac{m}{T_x} + \frac{n}{T_y} \right) \right) \right) H_{mn,pq}(k)]$$

Rigorous coupled wave analysis (RCWA)

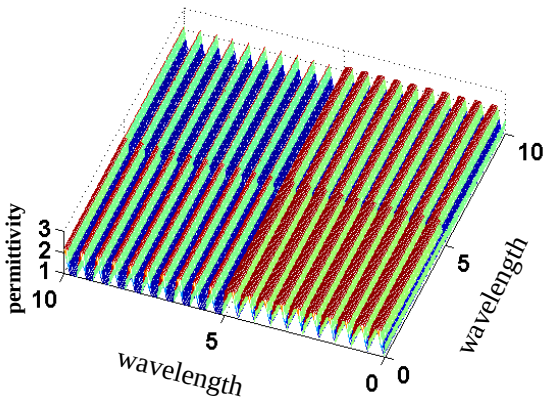

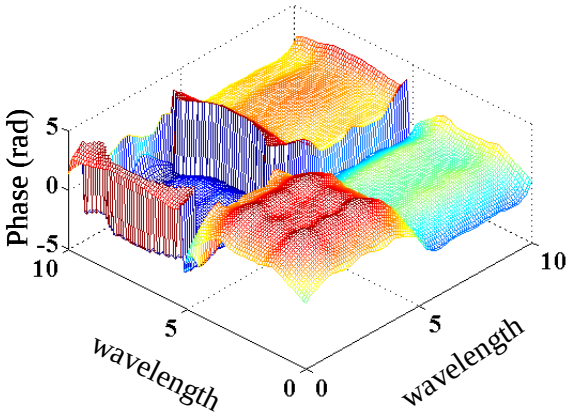

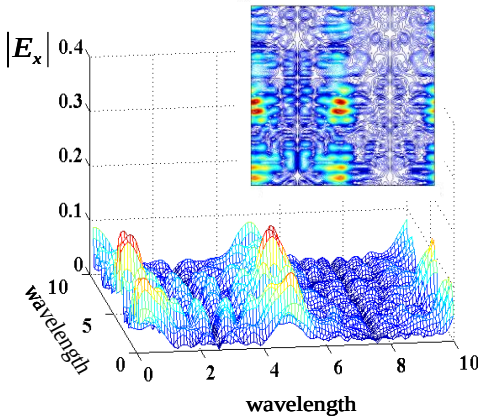

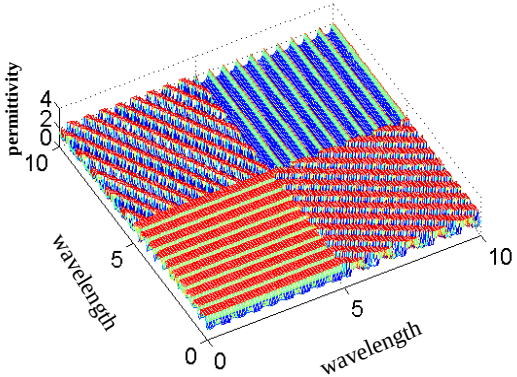

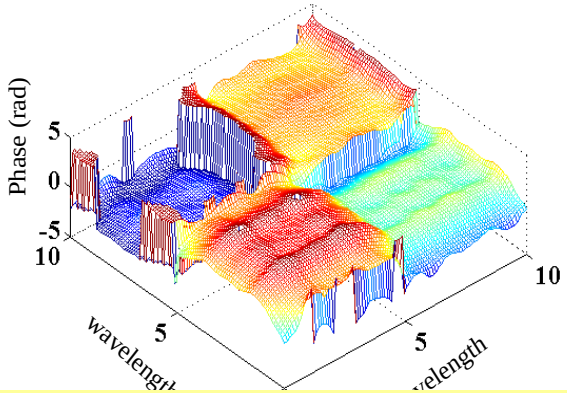

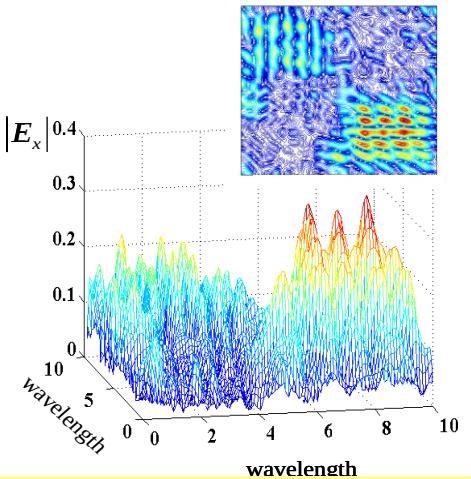

The binary subwavelength scale gratings can modulate both phase and amplitude of the incident optical field.

Dynamic range of phase and amplitude modulation for fill factor and tilt angle

Phase modulation

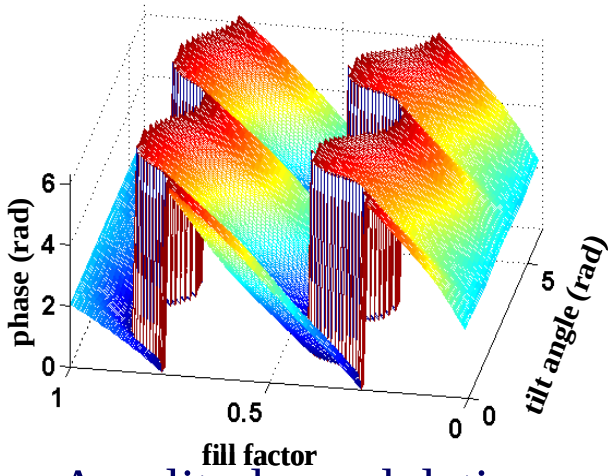

Amplitude modulation

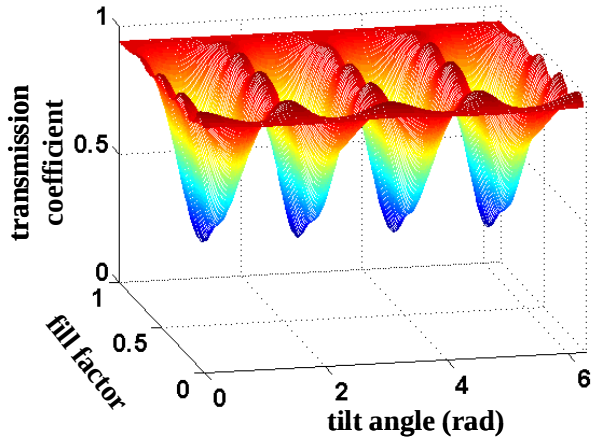

Dynamic range map in phase and amplitude modulation for fill factor and tilt angle

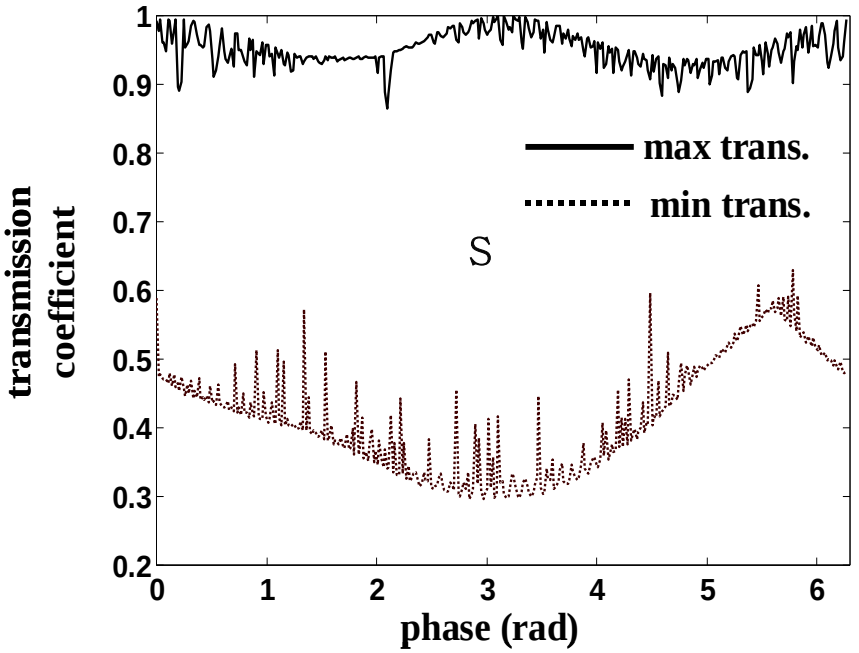

Beam shaping with a dynamic liquid crystal spatial light modulator

- **LC SLM beam shaping system (phase hologram)**

- Electrical controllability
- Real-time dynamic beam shaping

System layout

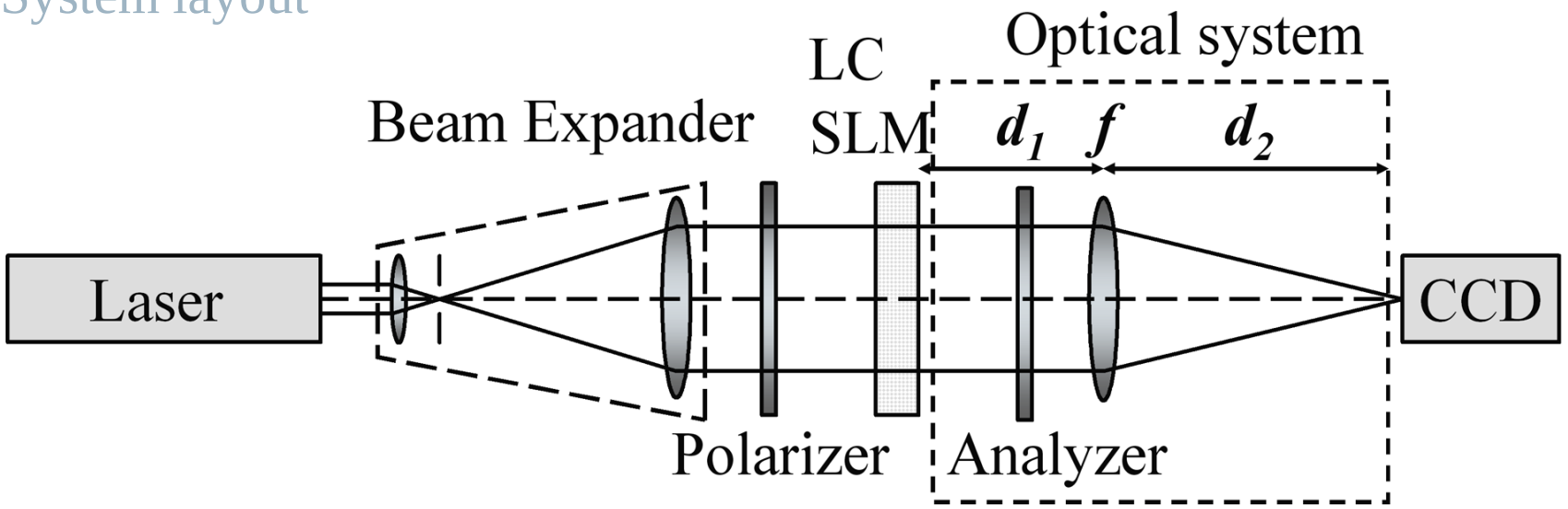

Phase and amplitude modulations of the LC SLM

- **Dynamic characteristics of LC SLM**

  Nonlinear variation of the phase and amplitude of the SLM

  Phase and amplitude compensation

These relationships must be taken into account in the phase hologram design.

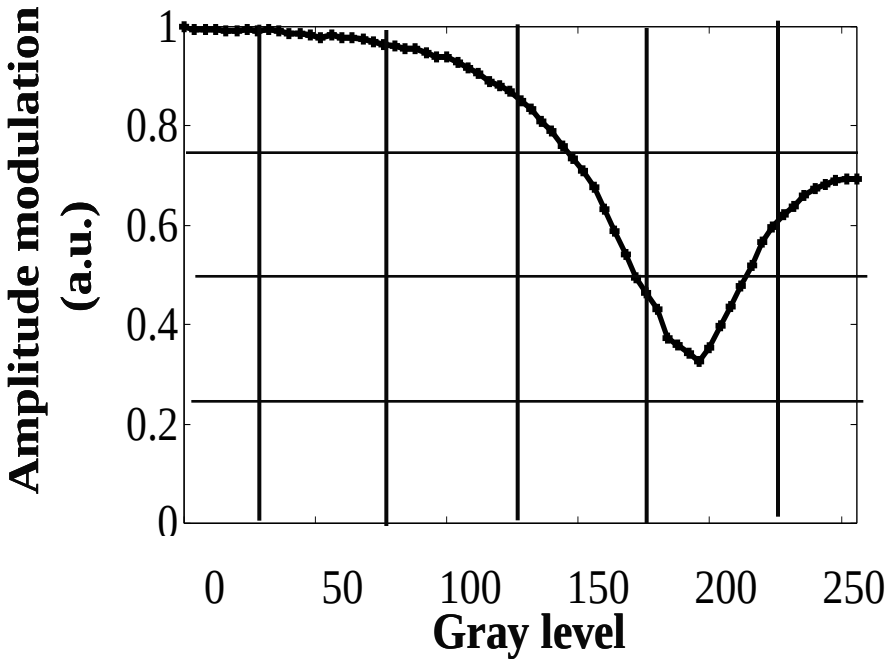

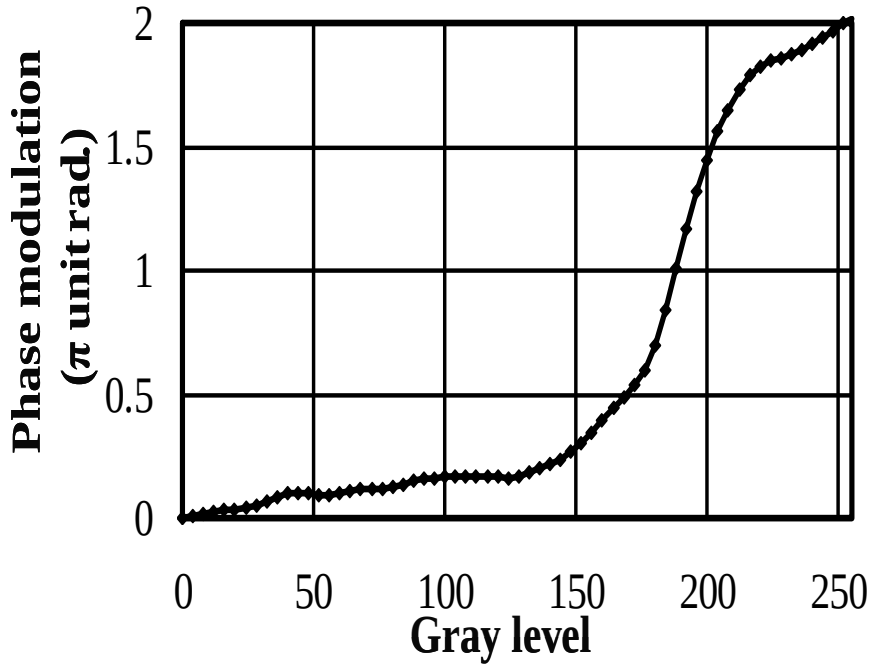

Beam shaping system with the genetic feedback tuning loop(GFTL)

- Experimental setup with real-time adaptive genetic feedback tuning loop

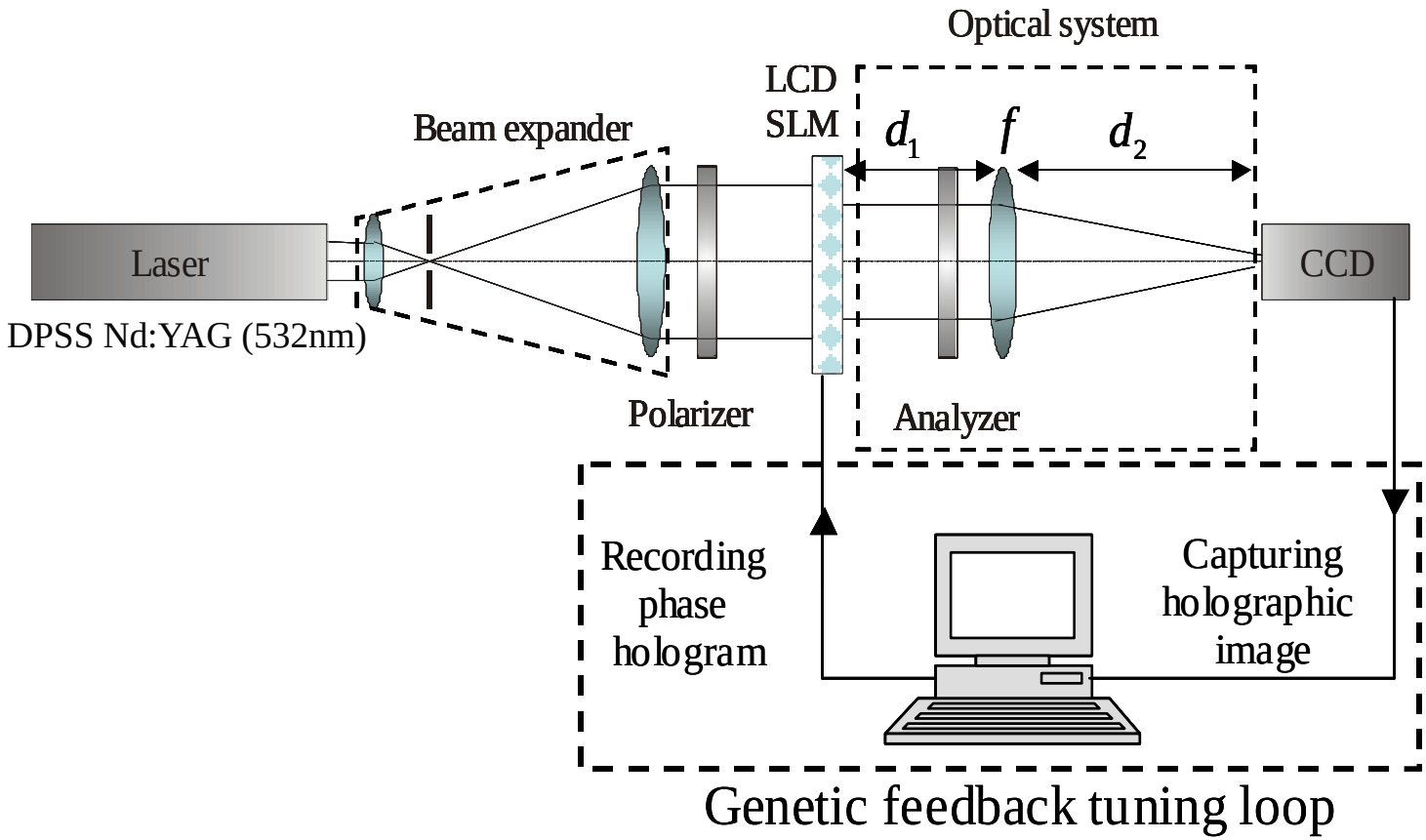

J. Hahn, H. Kim, K. Choi, and B. Lee, Applied Optics, vol. 45, no. 5. p. 915-924, 2006.

System control panel & implemented genetic algorithm

Control panel for adaptive beam shaping

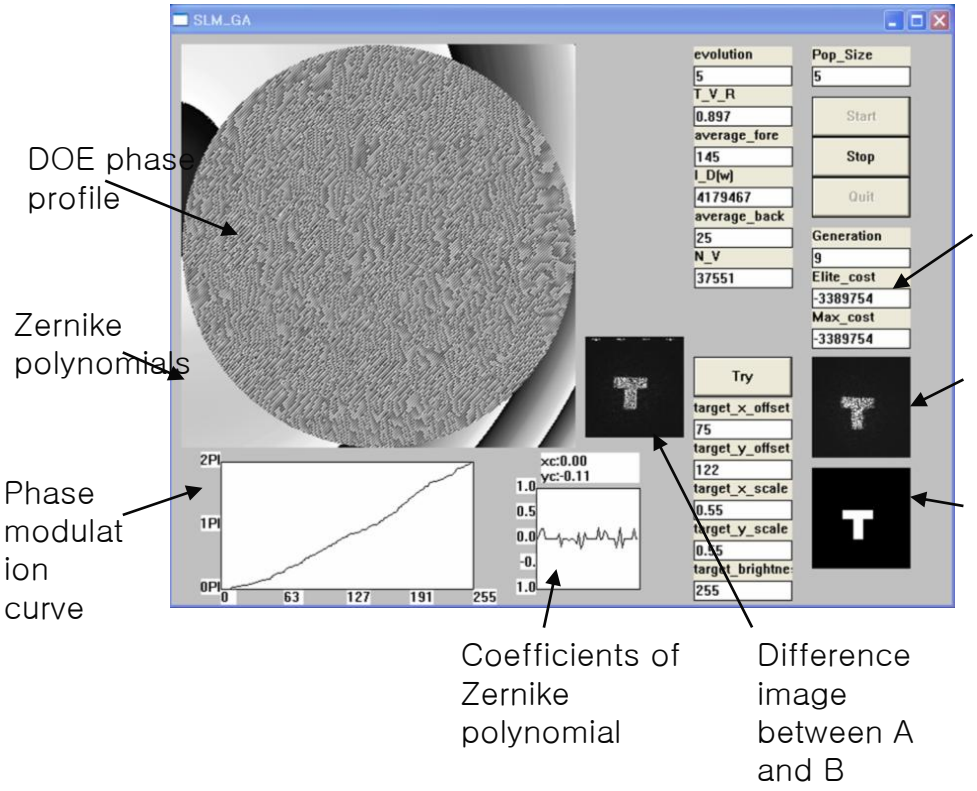

Genetic algorithm

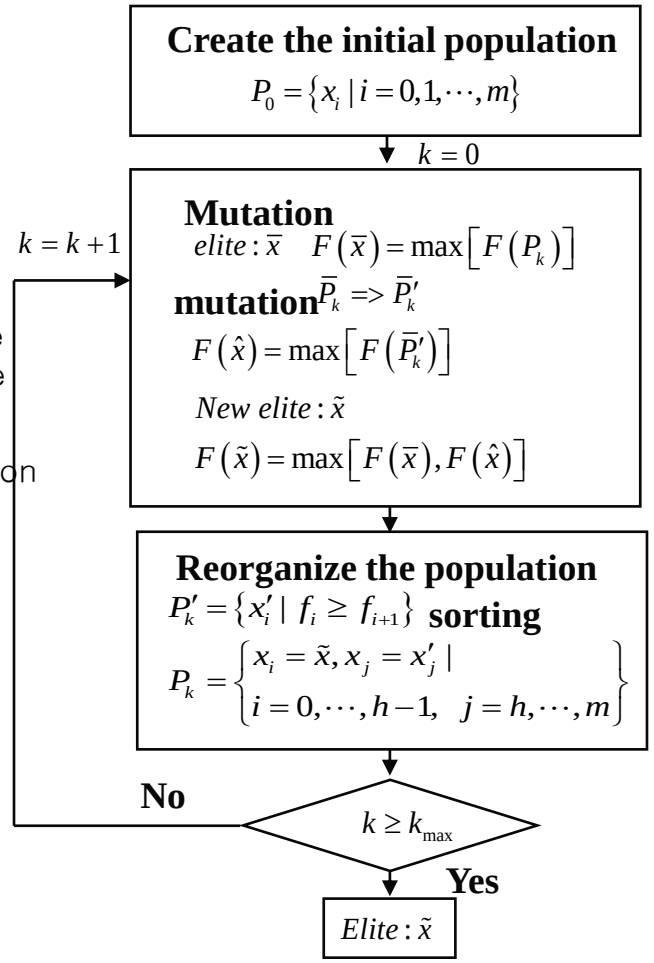

Aberration compensation in the GFTL beam shaping system

- Zernike polynomial model of compensating phase profile

$$\Omega(x,y)=\Omega(\rho,\theta)$$
$$=A_{00}+\frac{1}{\sqrt{2}}\sum_{n=2}^{\infty}A_{n0}R_n^0(\rho)+\sum_{n=1}^{\infty}\sum_{m=1}^{n}A_{nm}R_n^m(\rho)\cos m\theta+\sum_{n=1}^{\infty}\sum_{m=1}^{n}A'_{nm}R_n^m(\rho)\sin m\theta,$$

$$\rho=\sqrt{(x-x_c)^2+(y-y_c)^2}\qquad \theta=\tan^{-1}\left(\frac{y-y_c}{x-x_c}\right)$$

$R_n^m(\rho)$ Zernike polynomial

$\{A_{mn}\}$ coefficients to be optimized

The GFTL is effective in compensating the aberration of the internal optics of the beam shaping system.

Experimental setup

- Compensation of aberrated (tilted) optics with GFTL

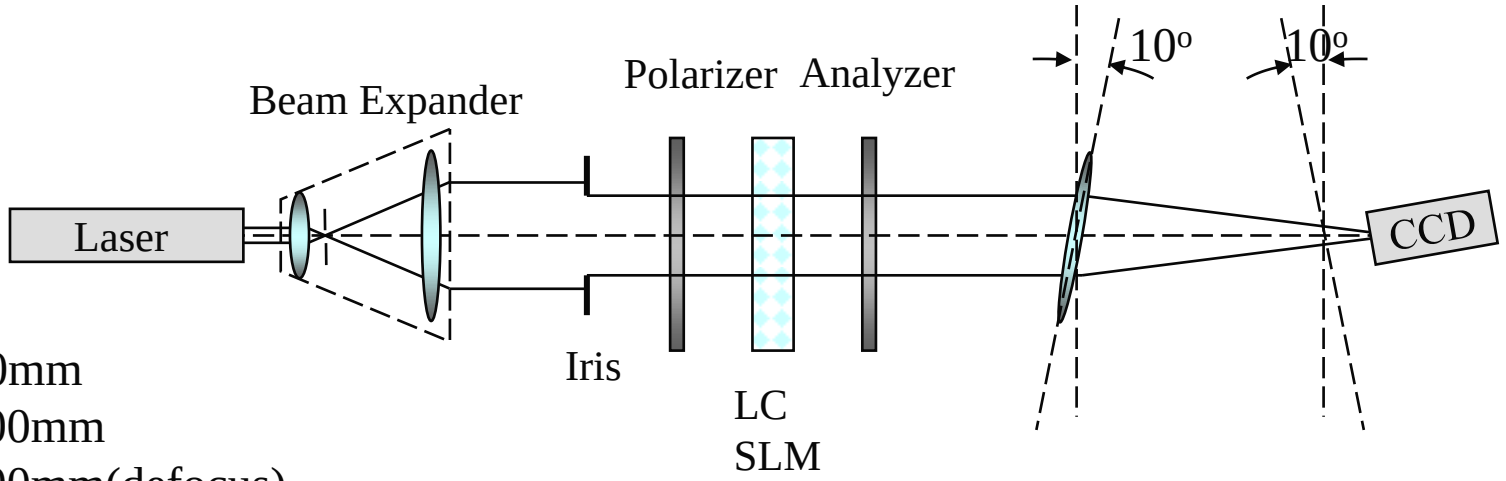

f = 500mm
d_1 = 500mm
d_2 = 490mm(defocus)
tilt angle of lens = +10°
tilt angle of CCD = -10°

Diffraction image obtained in the aligned optics

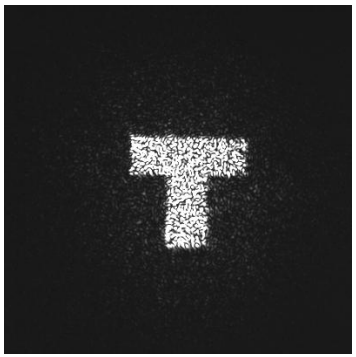

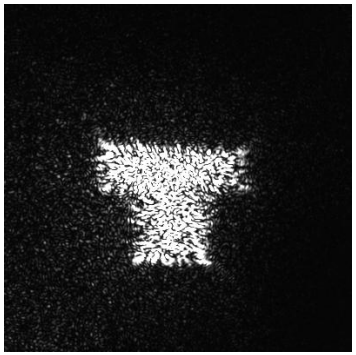

Distorted diffraction Image in the tilted optics

Experimental results – dynamic aberration compensation

Target diffraction image

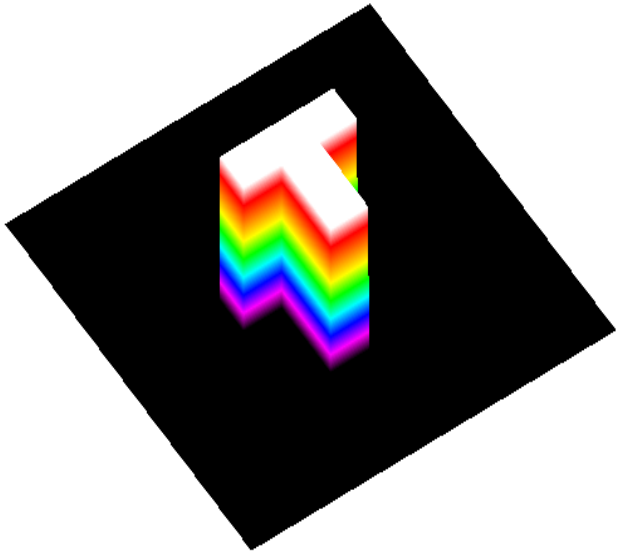

Evolution of
the diffraction image

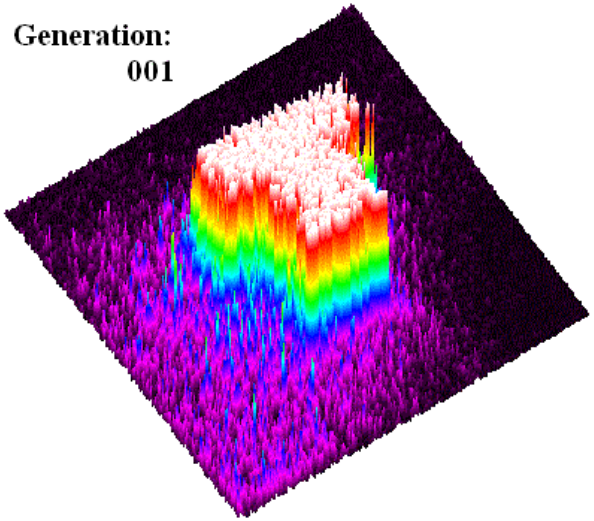

Resulting Zernike
phase profile

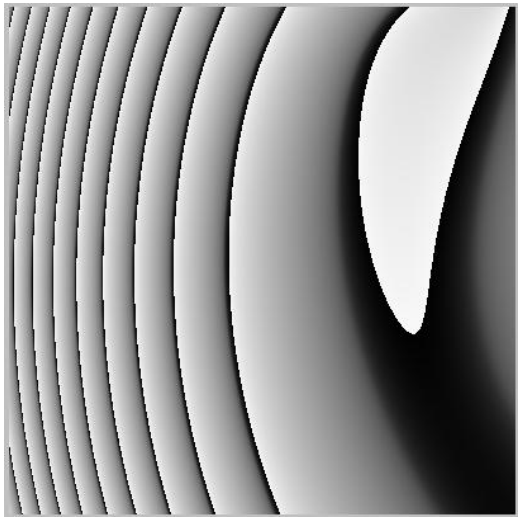

The diffraction image evolves to the target diffraction image, overcoming the internal aberration of the beam shaping system.

Experimental results – dynamic aberration compensation

Comparison of another diffraction image obtained by the compensated system in the previous page and the aberrated system

Aberrated diffraction image

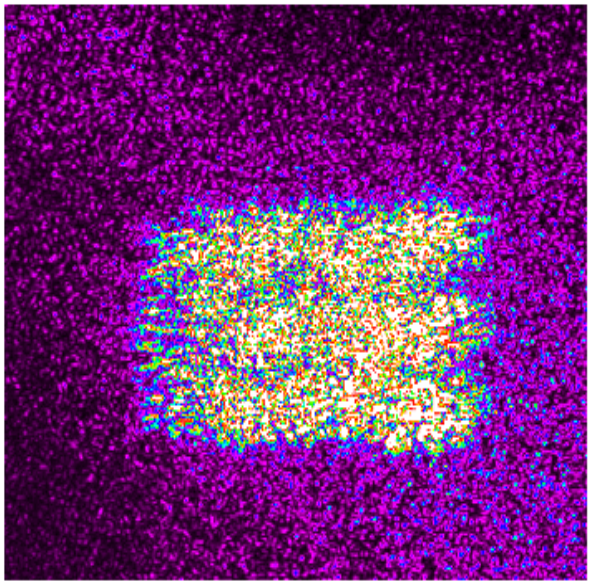

Compensated diffraction image

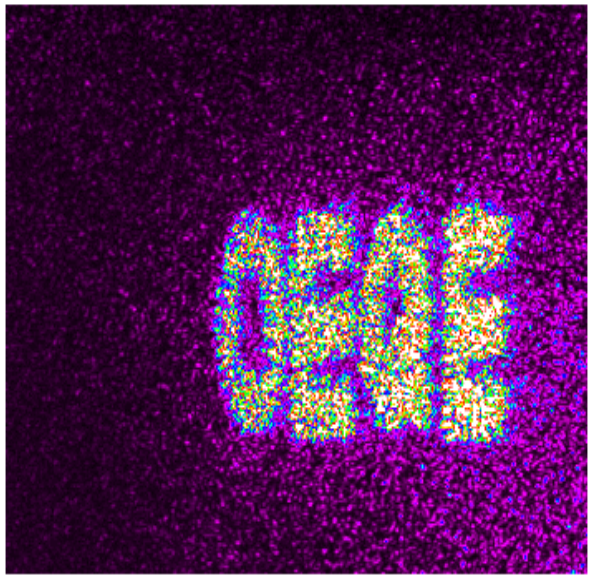

Reconfigurable 2D optical perfect shuffle network system

- 2-D perfect shuffle network system

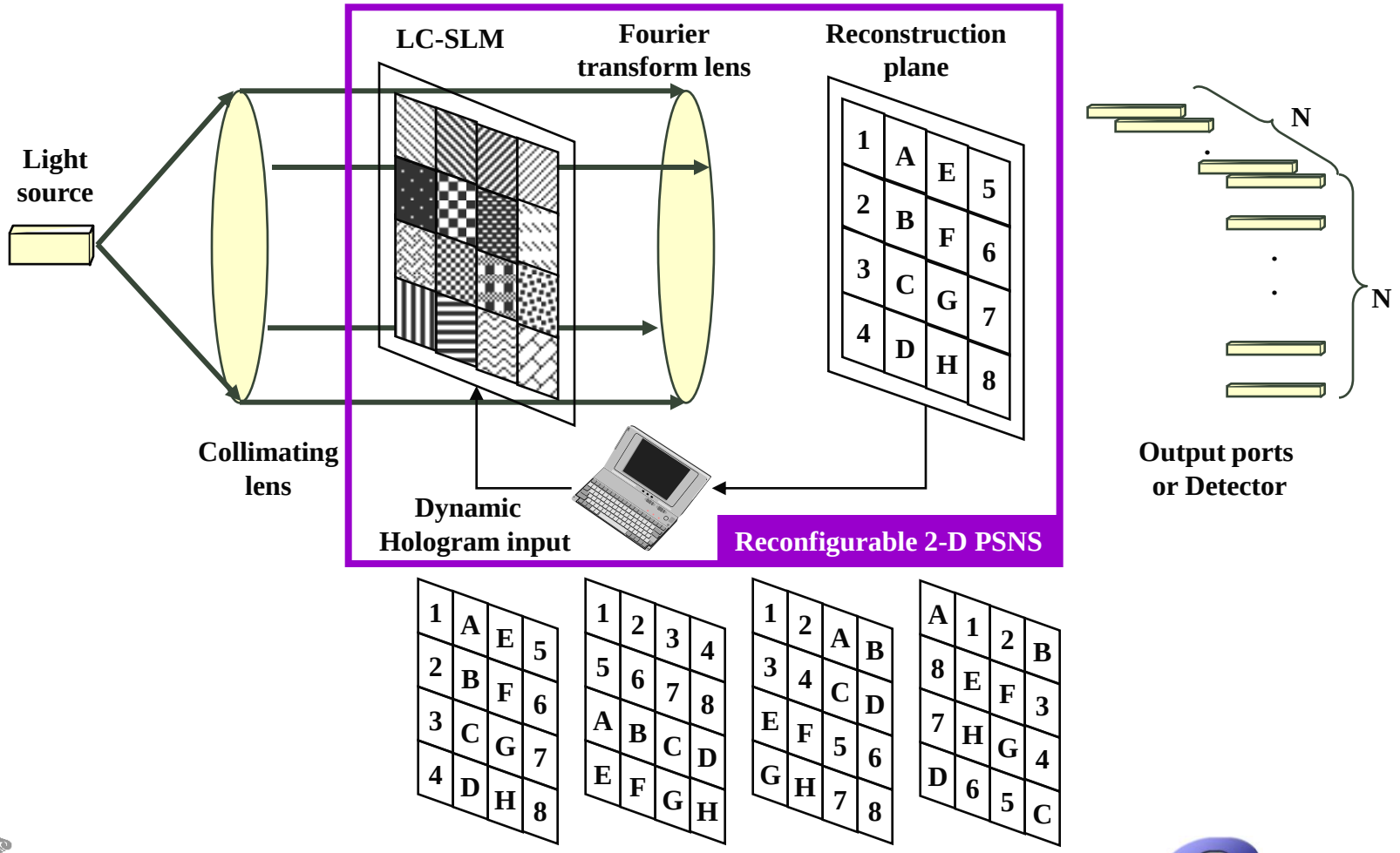

Experimental results

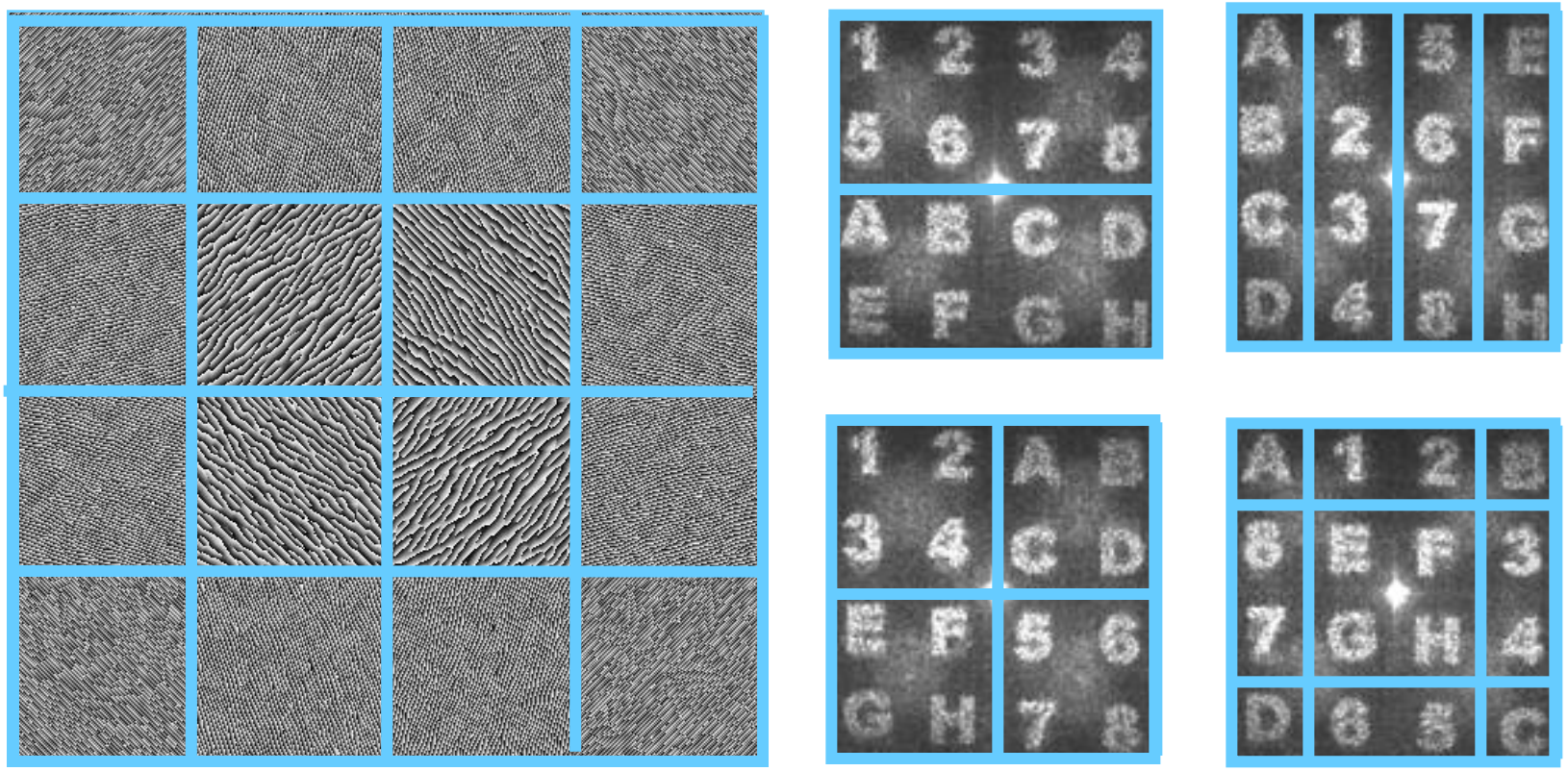

SLM: Holoeye Holo2002 832x624 (512x512) pixels, ~60 Hz maximum frame rate, 32um x 32 um pixel size

K. Choi and B. Lee, IEEE Photon. Technol. Lett., vol. 17, no. 3, p. 687, 2005.

Holographic optical tweezer

Laser tweezer setup and results

- λ_w = 532nm (Nd:YAG, 5W), Dielectric spheres (silica,8.6μm & polystylene, 6.7μm)
- Dynamic computer-generated hologram loaded on 2D spatial light modulator

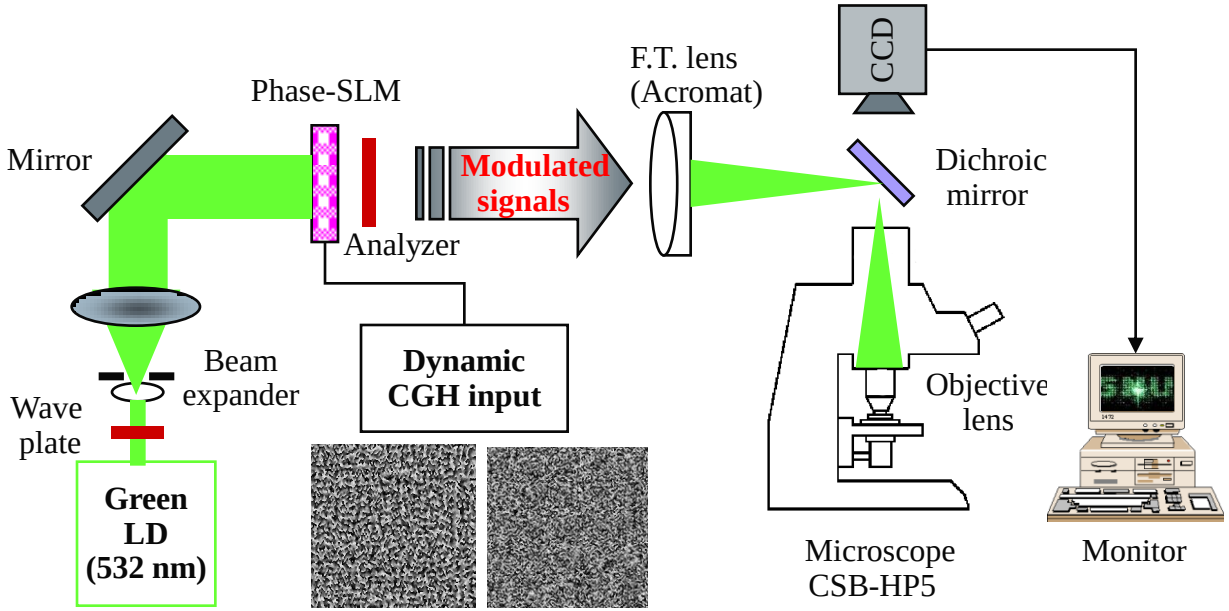

Diagram showing the optical setup of laser tweezers with dynamically controlled holograms of the laser beam

Experimental results

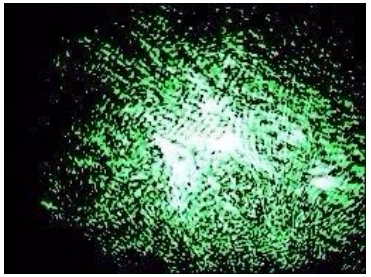

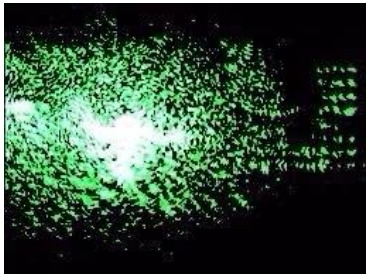

Scattering patterns

Full-color autostereoscopic 3D display system using color-dispersion compensated computer generated (CG) DOEs

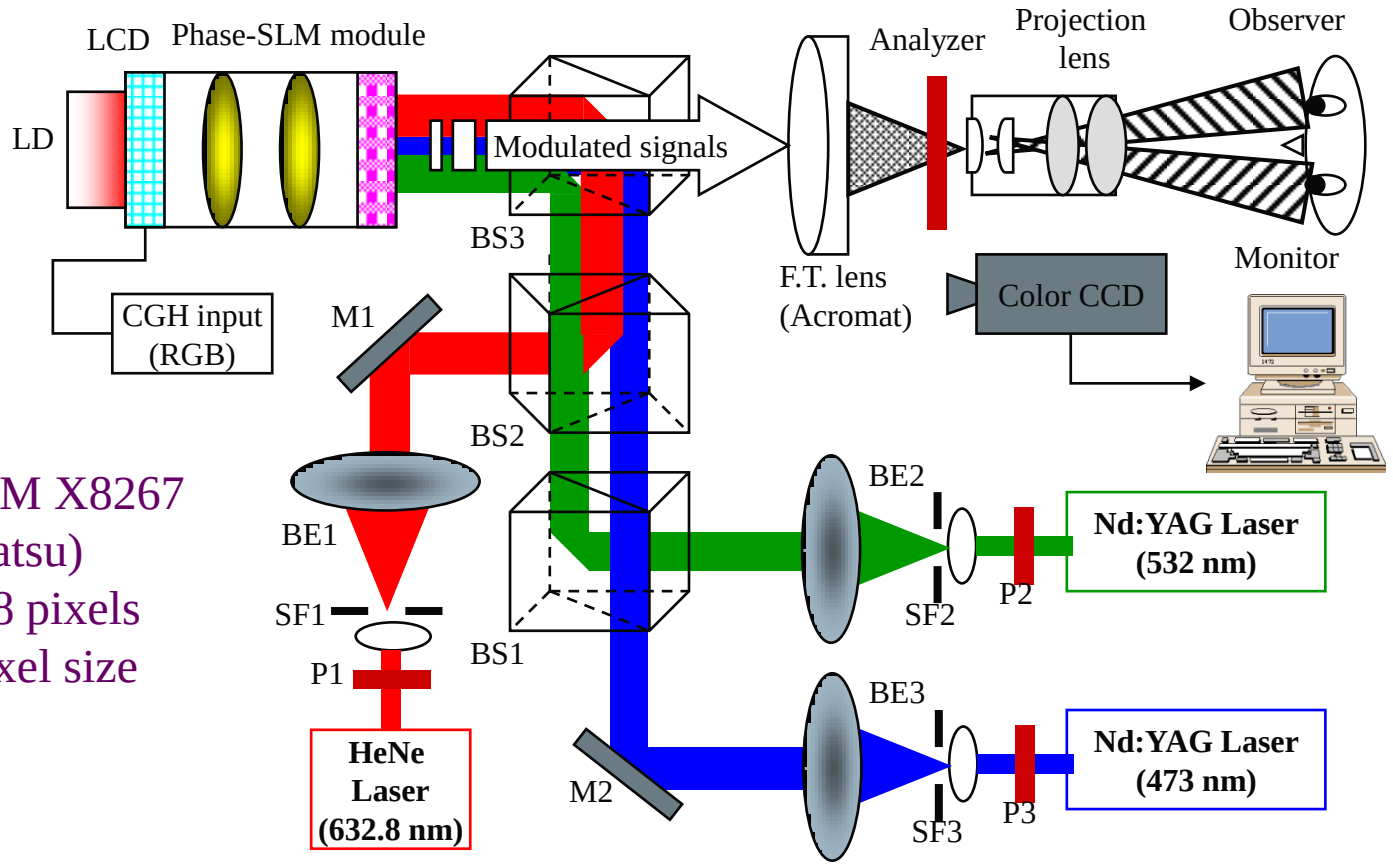

SLM: PPM X8267 (Hamamatsu)
1024x768 pixels
25 um pixel size

K. Choi, H. Kim, and B. Lee, Optics Express, vol. 12, no. 11, p. 2454, 2004.
K. Choi, H. Kim, and B. Lee, Optics Express, vol. 12, no. 21, p. 5229, 2004.

Simulation of full-color auto-stereoscopic video using CG-DOEs

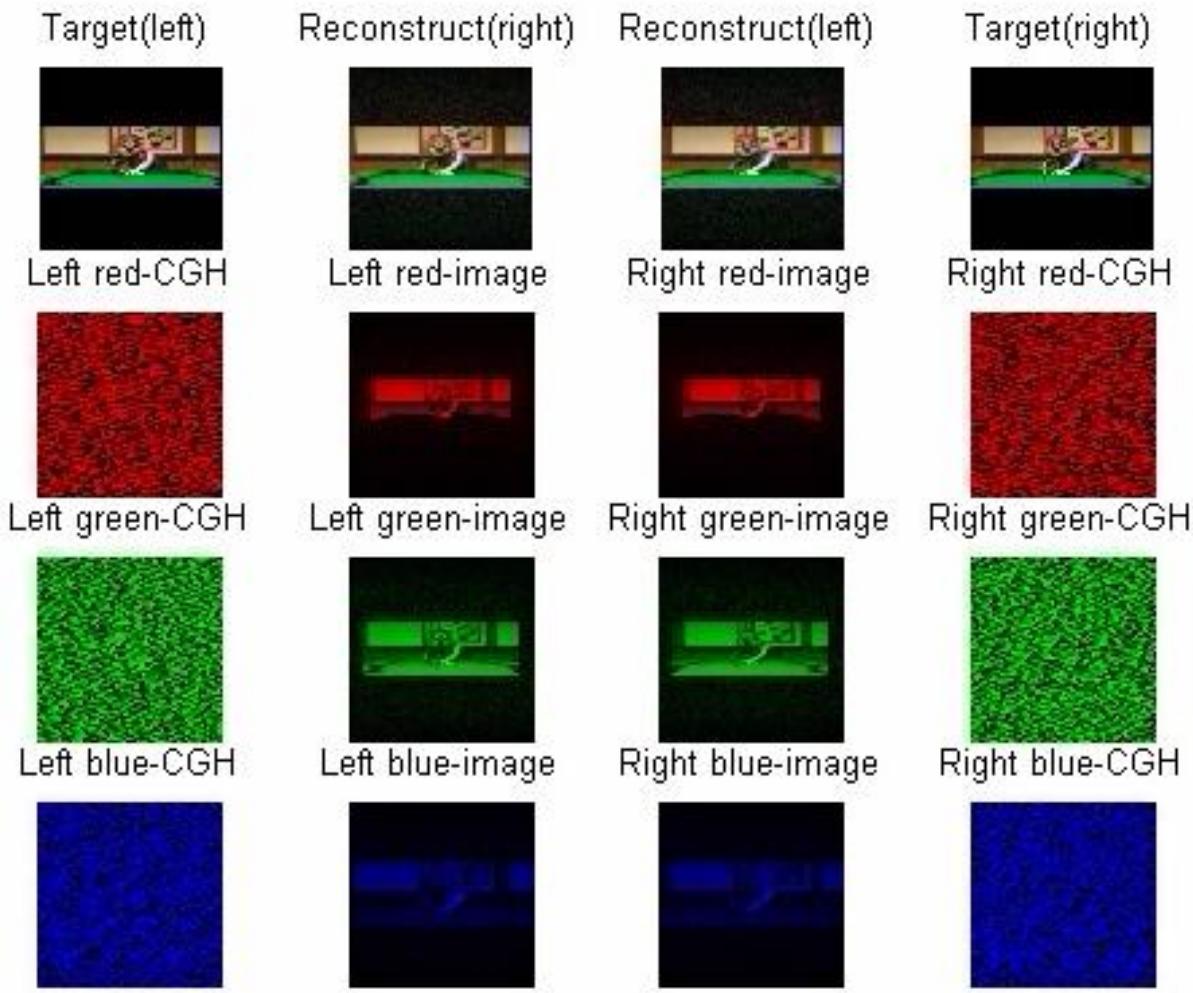

Demonstration system for full-color auto-stereoscopic 3D display using CG-DOEs

Full-color autostereoscopic 3D display demo system

Reconstructed stereo video (simulation)

Reconstructed stereo video (experiment)

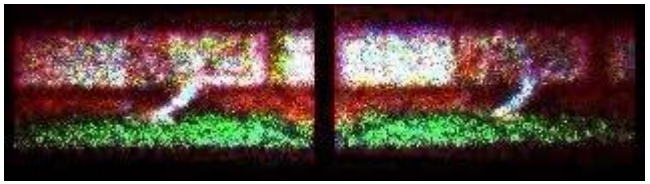

Stereo input video

Multi-view stereoscopic display system using CG-DOEs

- Schematic diagram of our multi-view auto-stereoscopic 3D display system

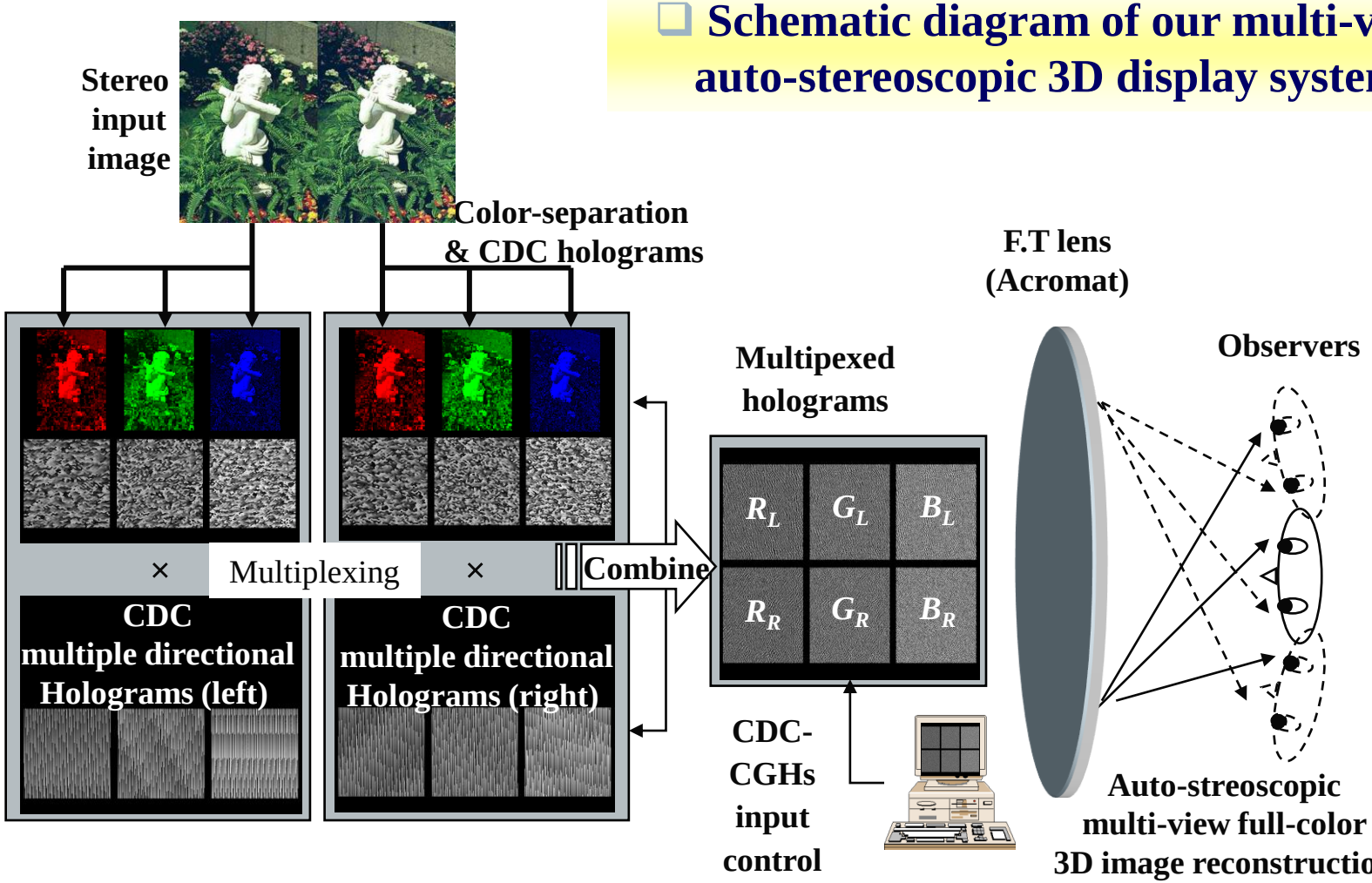

Schematic of multi-view stereoscopic display system using CG-DOEs

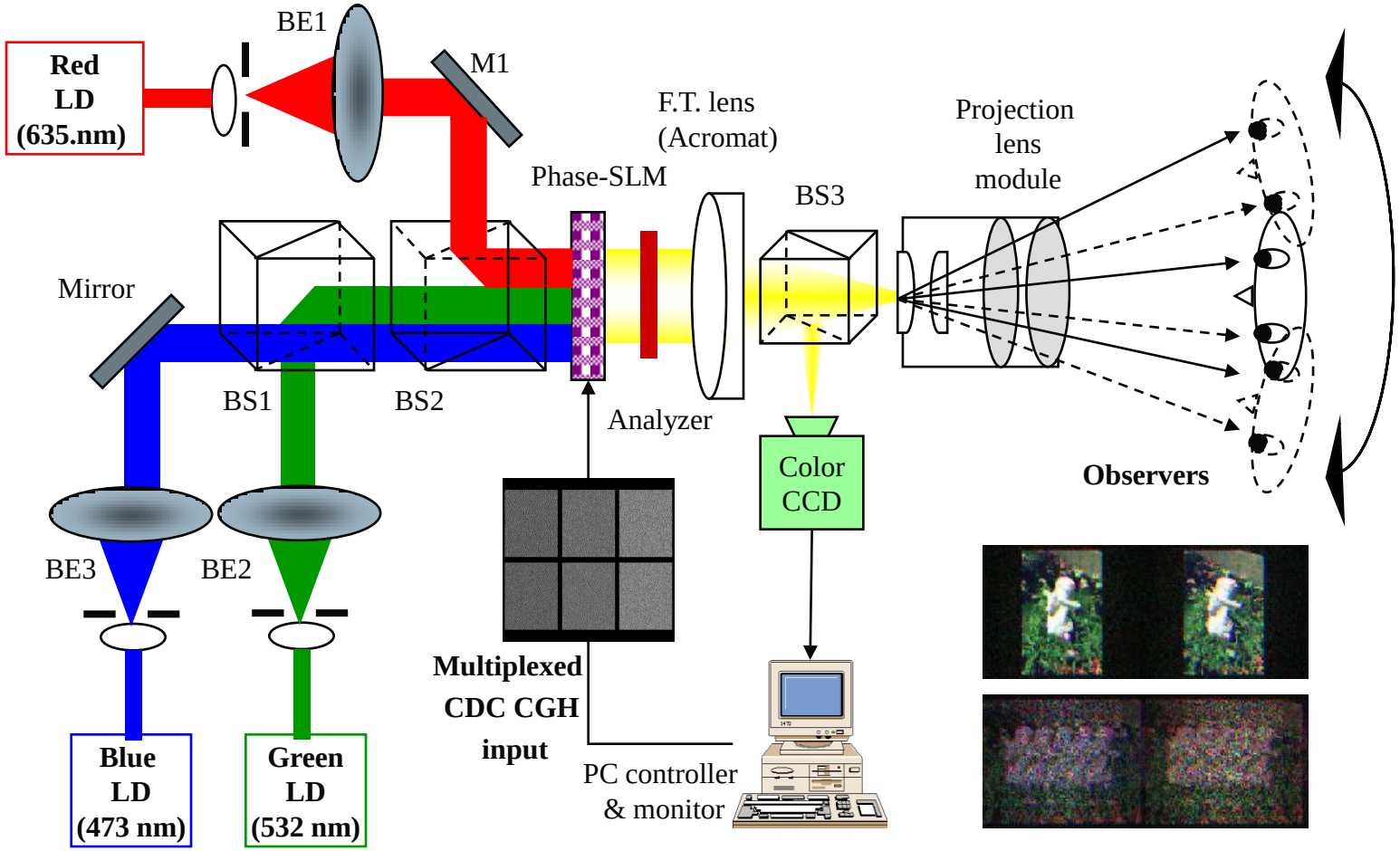

Full-parallax 3D display system using CG-DOEs and integral imaging

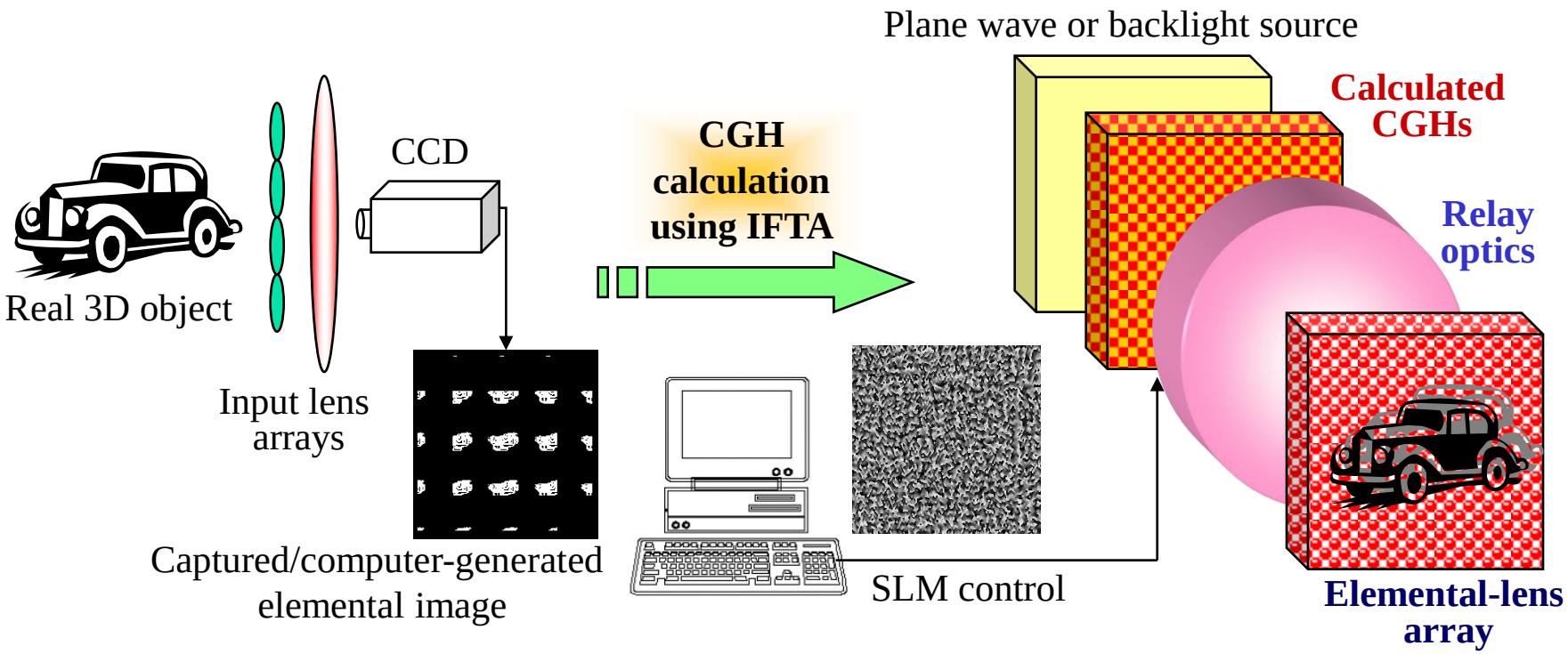

K. Choi, J. Kim, Y. Lim, and B. Lee, Optics Express, vol. 13, no. 26, pp. 10494-10502, 2005.

Full-parallax 3D display system using CGHs and integral imaging

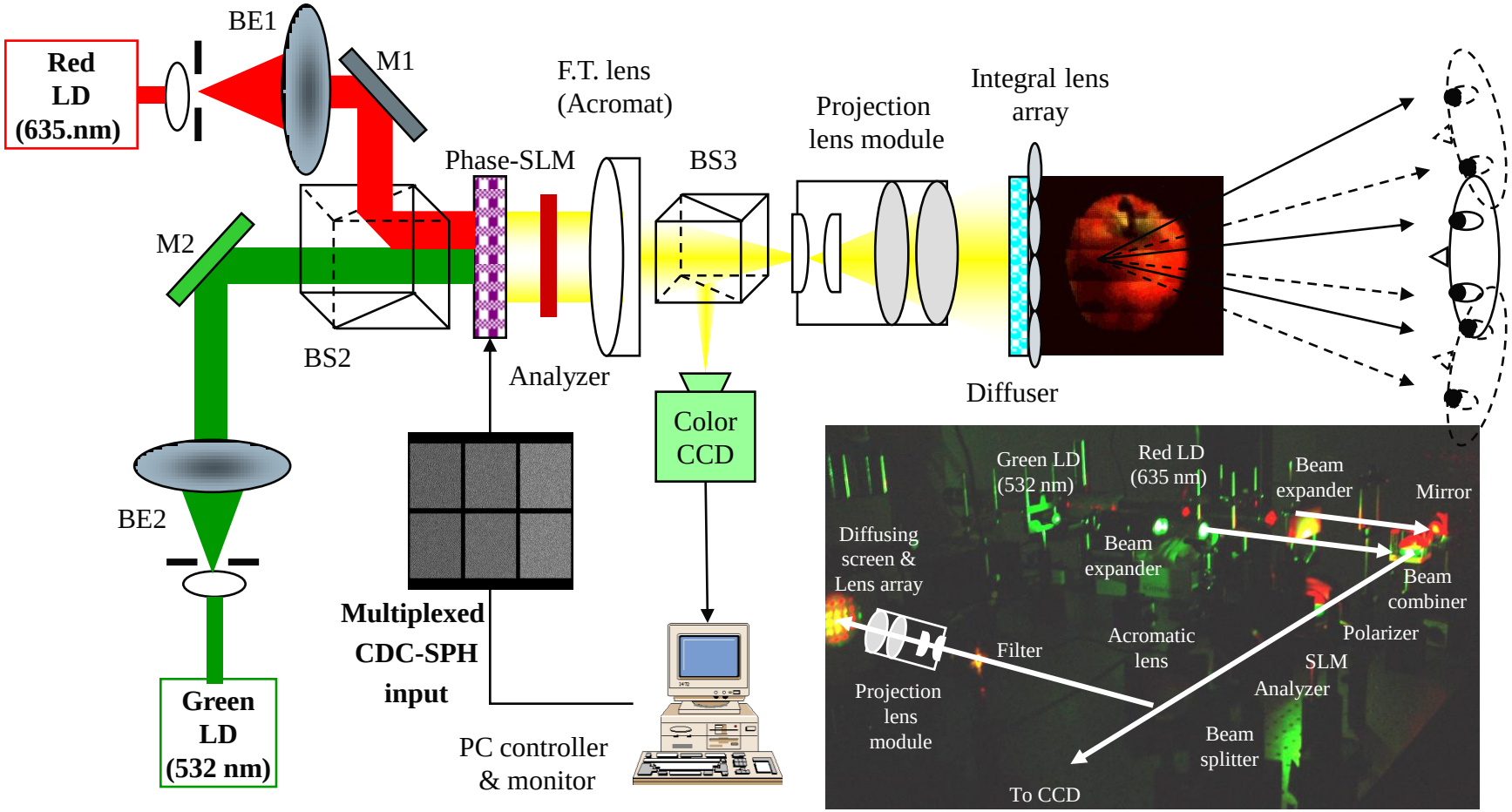

Experimental results

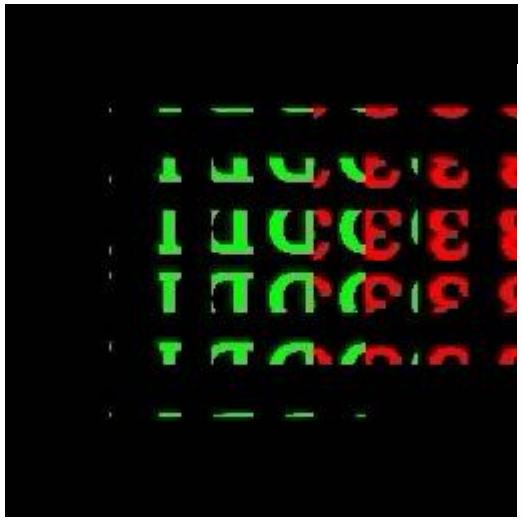

Elemental image input

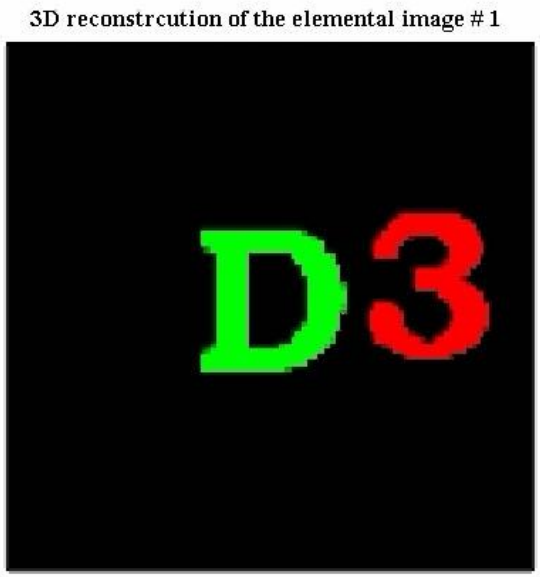

Reconstructed video (simulation)

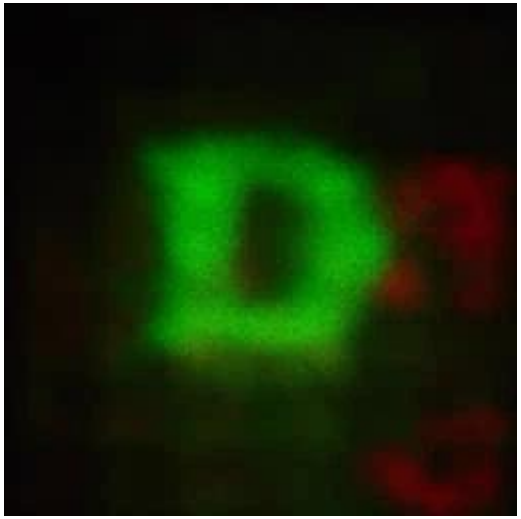

Reconstructed video (experimental result)

Brightness Enhancement Films

- Our surface relief structure for brightness enhancement films (BEFs)

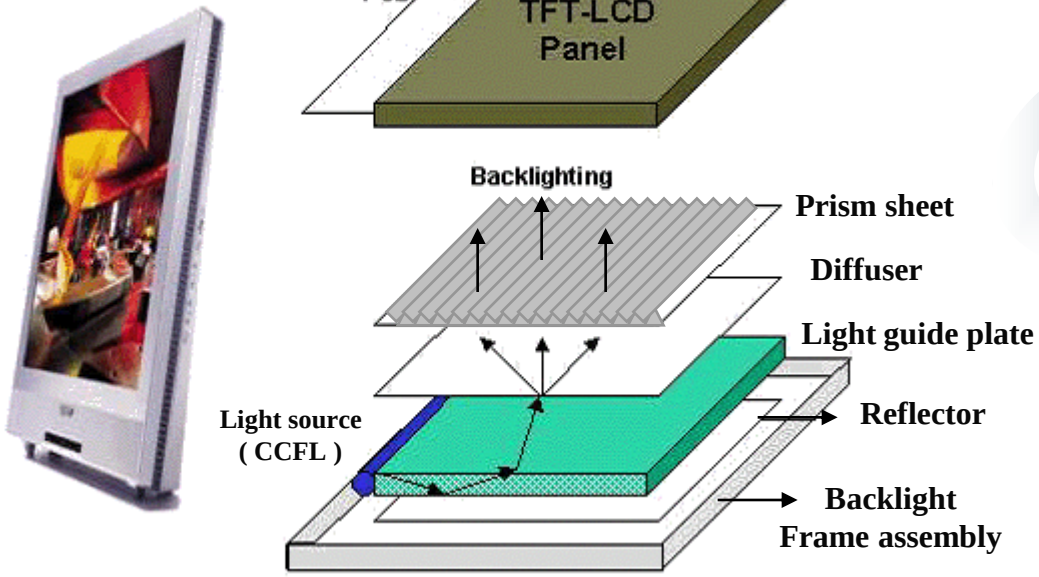

TFT-LCD backlight module structure

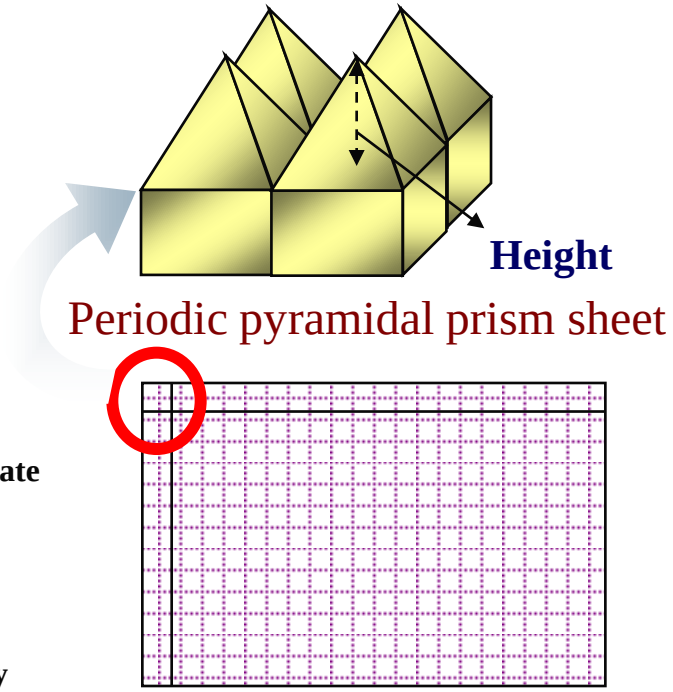

Our surface relief structure for substitution of prism sheet

Ray Tracing Simulation

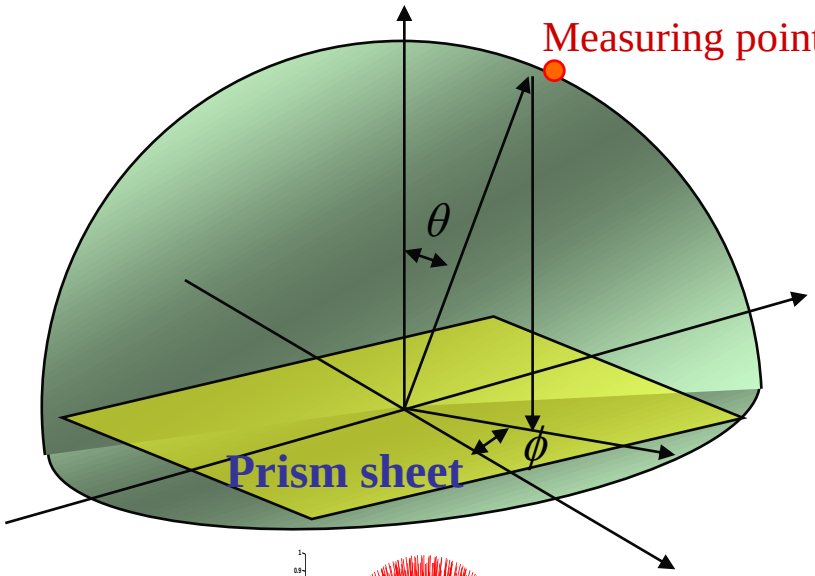

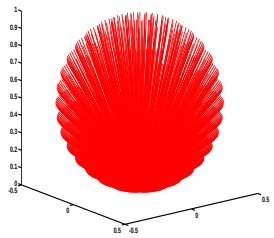

Radiant intensity of point source:

$$I(\theta,\phi) = B\cos\theta$$

- Uniformly distributed point sources
- Considering multiple ray scattering process on the surface
- Infinite size of prism sheet
- Periodic structure

Radiant intensity profile of uniform input , height of 0.7

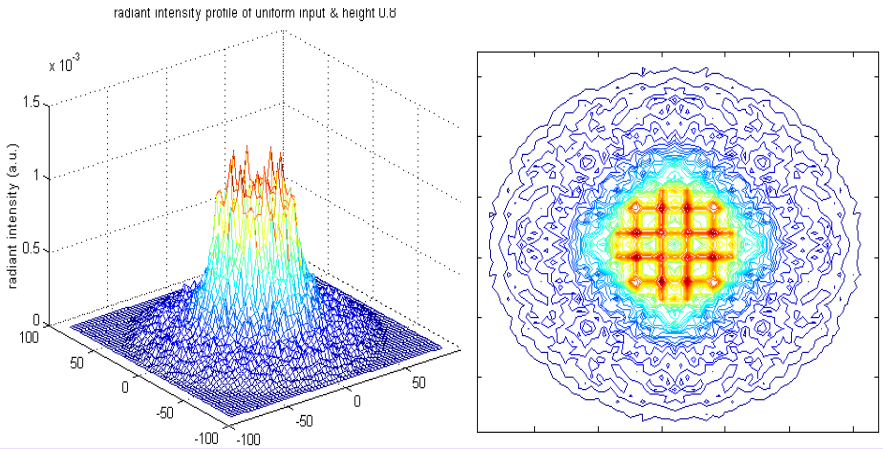

Classification of Rays Concentrated onto the Condensing Area by the Spatial Ray Directions

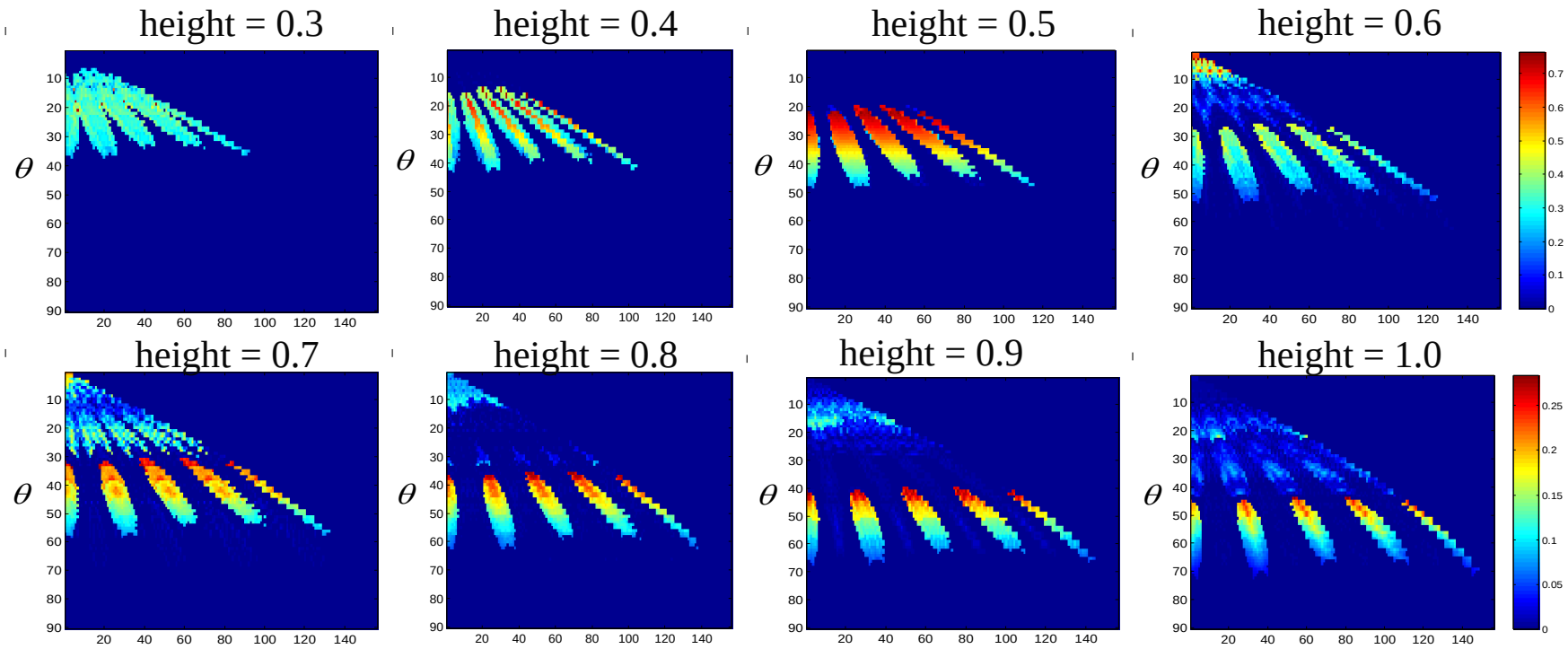

B. Lee, H. Kim, and K. Choi, "Design and analysis of gratings and diffractive optical elements for displays," Proc. The 5th Pacific Rim Conference on Lasers and Electro-Optics (CLEO/PR), Taipei, Taiwan, vol. 2, p. 643, CD file Paper TH4E-(17)-2, Dec. 2003 (Invited paper).

Engineered Diffusers™
- Random Microlens Screen Design Concept

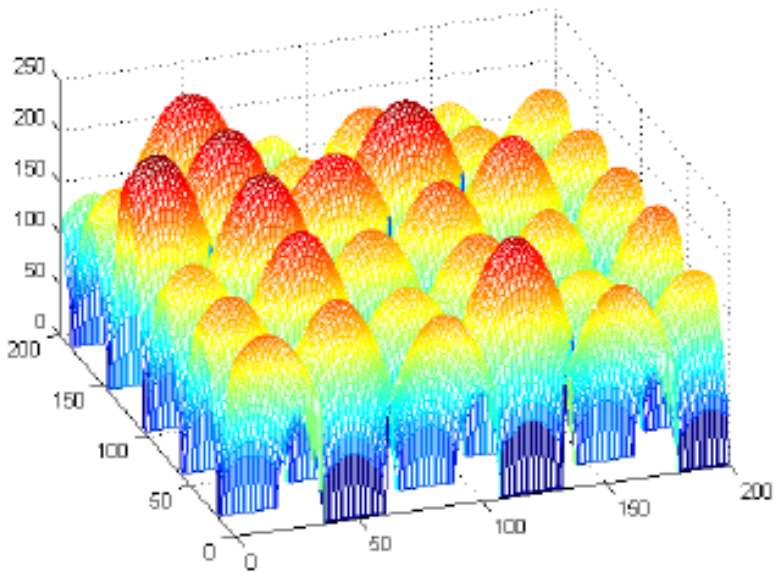

Random Microlens Array

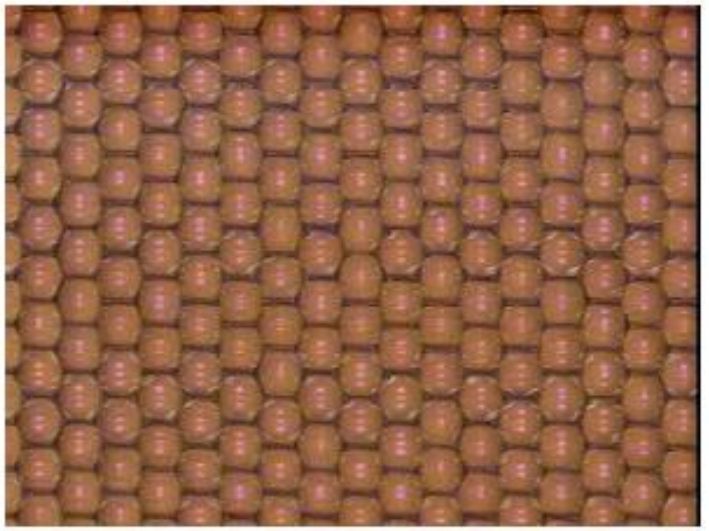

Photoresist Master

*** Figures are from the talk delivered by G. M. Morris in 2003.**

Full-Color Laser Display System

- Full-color laser display system using DOEs
  - ✓ Color optimization
  - ✓ $C_{min} = |\lambda(R) - N(R)| + |\lambda(G) - N(G)| + |\lambda(B) - N(B)|$
  - ✓ $N(R):N(G):N(B)$
    - $= (166 : 135 : 128)$
    - $= (262 : 213 : 202)$
    - $= (380 : 309 : 293)$

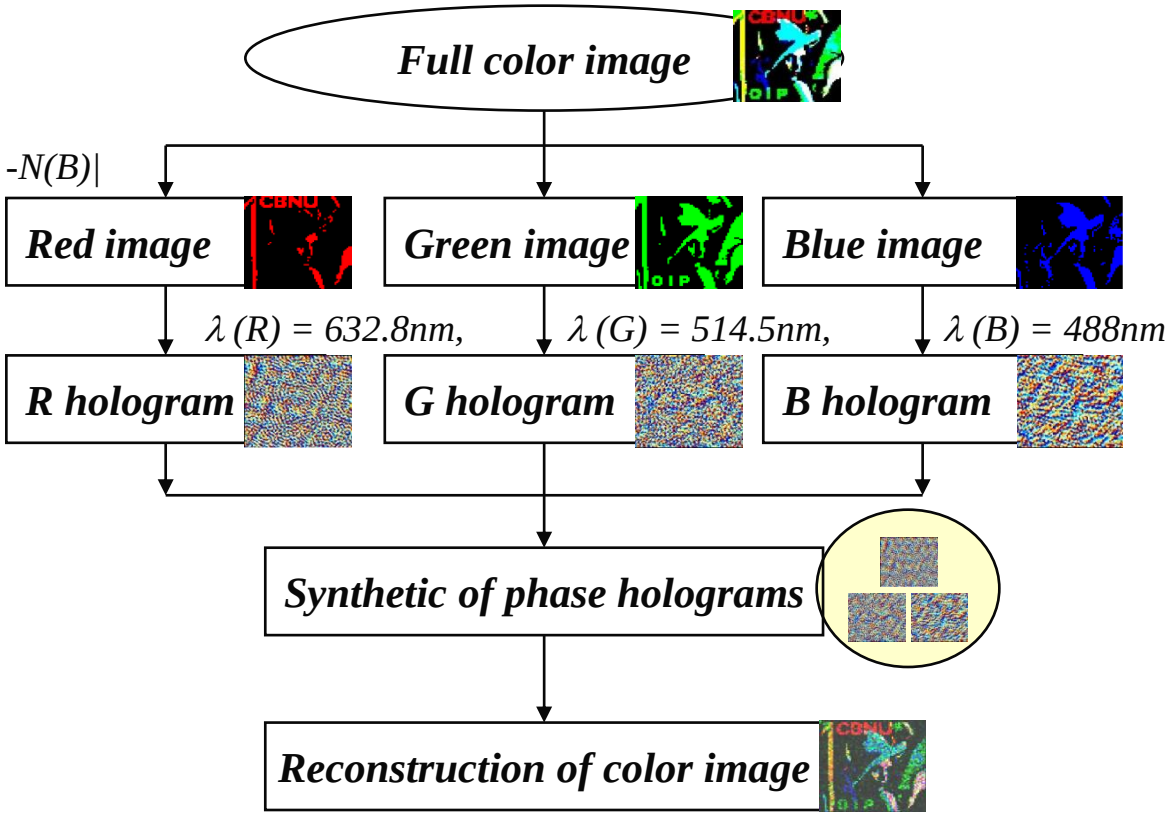

Principles of CDC-SPHs

- Principles of chromatic-dispersion-compensated synthetic phase holograms(SPHs)
  - ✓ Stereo viewing conditions
    - Observer's viewing distance (300mm), eye separation (65mm), pupil size (3mm).
    - Three illumination sources: 635nm (red), 532nm (green), and 473nm (blue)
    - The size of designed CDC-SPHs is 256X256 and minimum pixel size of SLM is about 32mm
    - Each size of reconstructed color image is about 6mm(R), 5mm(G), and 4.4mm(B)

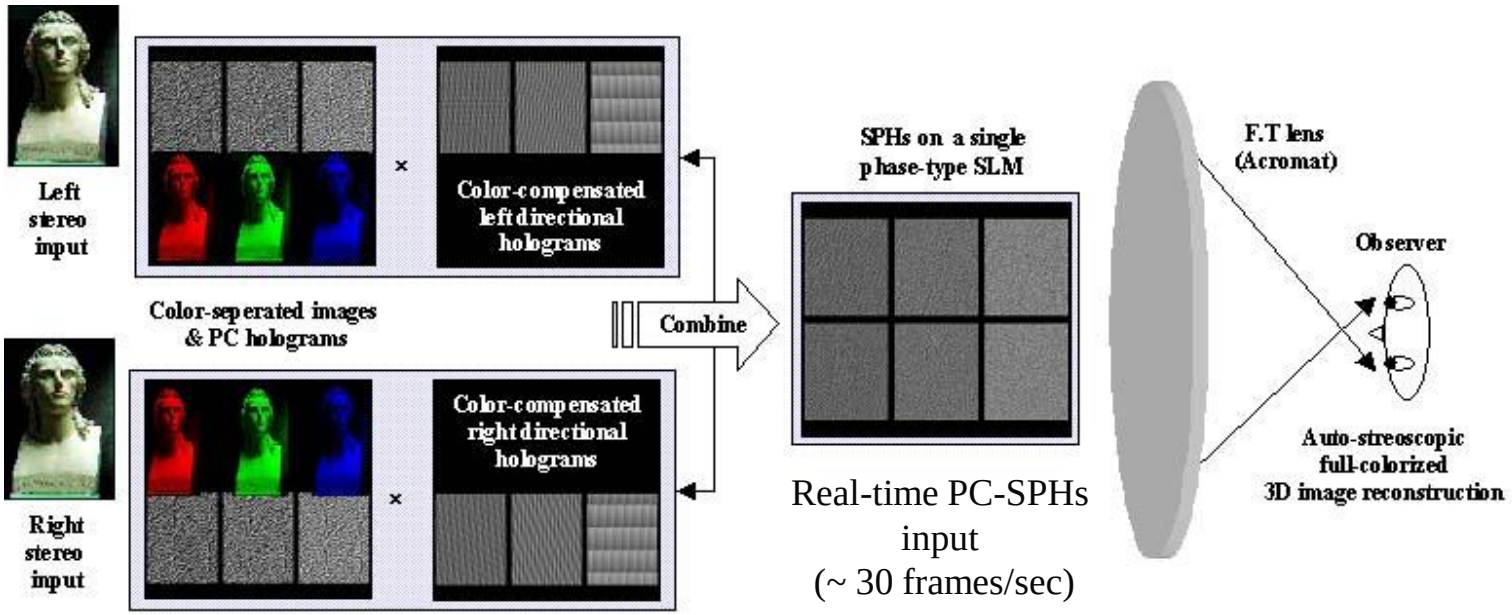

Experimental Setup and Results

- Experimental setup and results for the full-color CDC-SPHs
  - ✓ Dynamic full-color holographic display system using only a SLM and three sources
    - – The lens of the system must be an aberration-corrected(chromatic, spherical).

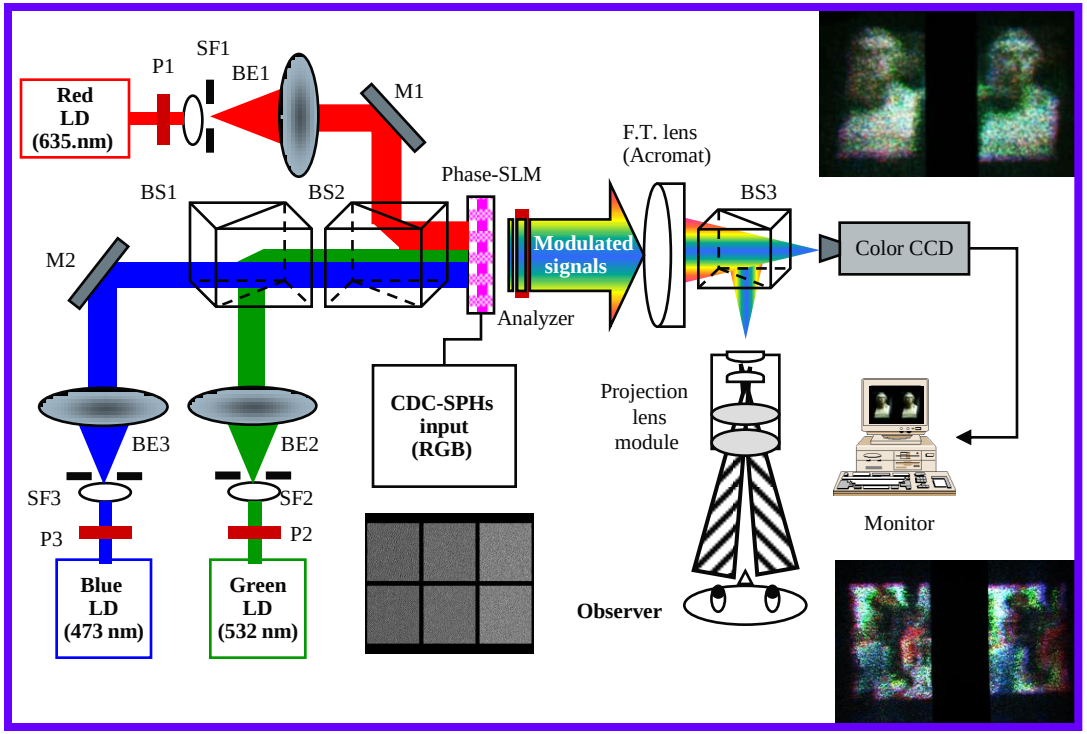

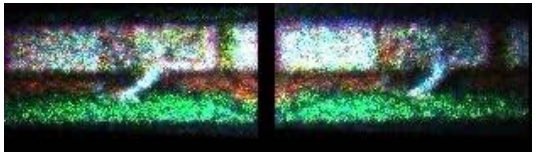

DOE Trend

Period	Driving force	Applications
Late 1980's ~early 1990's	The optical computing	▪ Back-plane optical interconnections ▪ Free-space 2D multi-plane optical interconnection architectures for 2D or 3D parallel optoelectronic processors ▪ 2D image processing applications ▪ Harmonic component filters → None of these optical functions are implemented in commercial architectures
Mid 1990's~	The optical storage	▪ Diffractive optical pick up units ▪ High NA diffractive lenses for magneto optical drives ▪ Beam splitting gratings for CD tracking ▪ DVD/CD lenses
Late 1990's	The optical telecom	▪ High order ruled gratings for WDM/DWDM Mux/Demux ▪ Micro Fresnel lenses for fiber couplers ▪ Diffractive microlens arrays for 10Gb/s

Continued..

Period	Driving force	Applications
Current	▪ Anti-counterfeiting market ▪ Imaging applications ▪ Ophthalmic industry ▪ Photographic industry ▪ Personal digital accessory and consumer electronics technology ▪ Optical metrology ▪ Entertainment business-packaging industry	▪ Diffractive optical variable image devices ▪ ID cards ▪ Virtual keyboard projector ▪ Laser radar motion sensing devices ▪ Hybrid zoom lens objectives using pairs of sandwiched diffractives ▪ Subwavelength diffractive elements polarization beam splitting anti-reflection surfaces for solar cells, polarization sensitive and high resolution ▪ Resonance filtering applications ▪ Laser pointer pattern generator
Future	Biotechnology High resolution lithography	▪ Fluorescence measurement ▪ Optimum reticle illumination ▪ Complex phase shift mask

Conclusion-DOE

- Concepts of DOE and some applications

- Theory and design issues of DOEs are introduced and discussed.
  - ✓ Scheduling relaxation parameters of IFTA
  - ✓ Modulation of both phase and amplitude of optical wave by using binary surface relief structure on a sub-wavelength scale
  - ✓ Boundary-modulated DOE optimization

- Display application examples using DOEs are presented.
  - ✓ Light condensing characteristics of a periodic pyramidal prism sheet
  - ✓ Full-color laser display system using DOEs
  - ✓ Directional DOEs for LCD-based stereoscopic systems